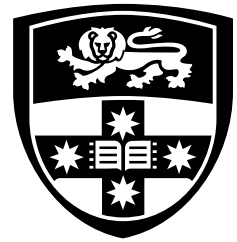

THE UNIVERSITY OF SYDNEY

Probing the cosmic dipole in the radio sky

RACS-low and NVSS

Oliver Oayda

PhD Candidate
Sydney Institute for Astronomy
The University of Sydney

Supervised by
Geraint Lewis
Tara Murphy

August 14, 2024

Agenda

- Background
  - The Cosmological Principle
  - CMB (Kinematic) Dipole
  - Testing the Principle
  - Literature Results
- Analysis
  - Samples
  - Preparation
  - Statistics
- Results
  - Individual
  - Joint
  - Local Sources
- Conclusions

Background

The Cosmological Principle

On very large scales, the Universe looks the same everywhere — it is homogeneous and isotropic.

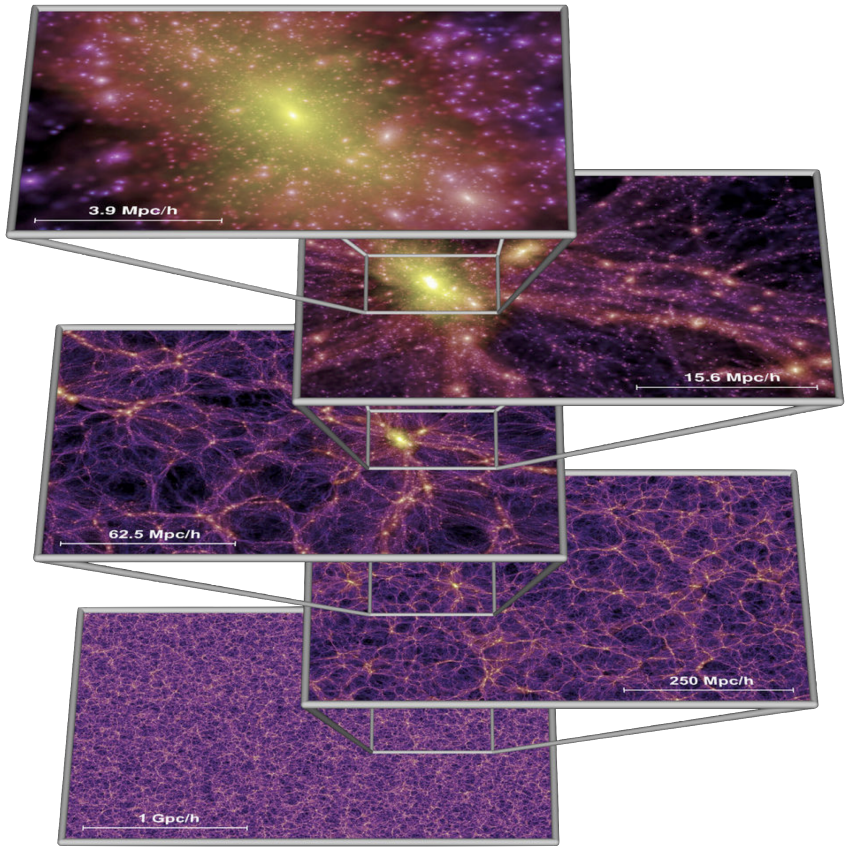

Figure 1: Millennium dark matter simulation (Springel et al., 2005).

The Cosmological Principle

On very large scales, the Universe looks the same everywhere — it is homogeneous and isotropic.

Foundational assumption in current cosmological framework, e.g. FLRW, Friedmann world models, etc.

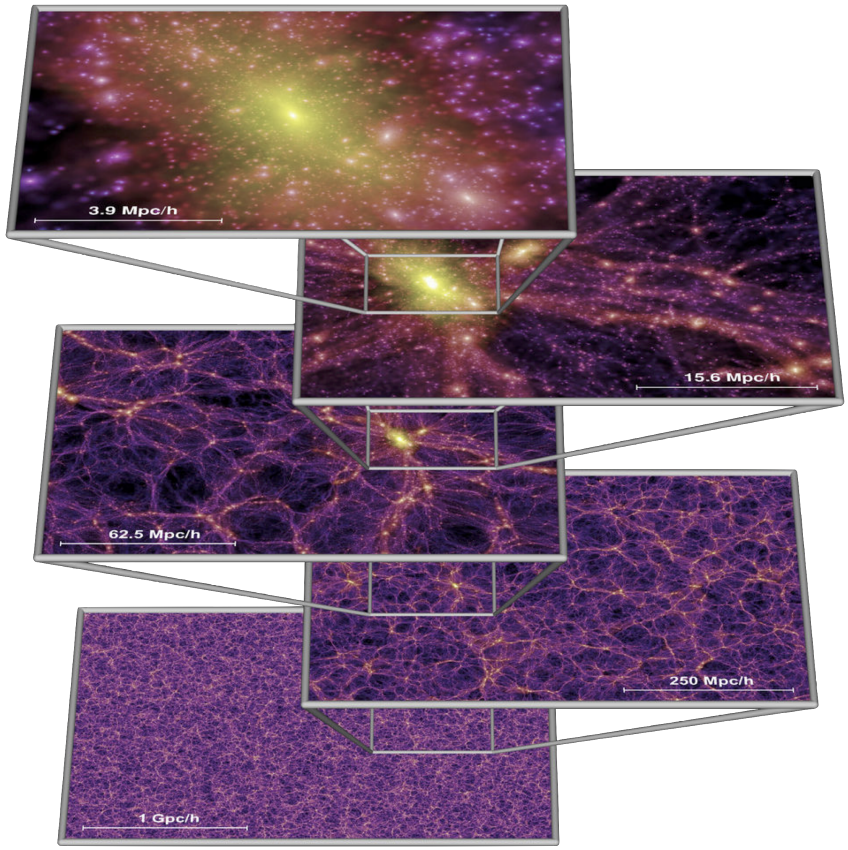

Figure 1: Millennium dark matter simulation (Springel et al., 2005).

The Cosmological Principle

On very large scales, the Universe looks the same everywhere — it is homogeneous and isotropic.

Foundational assumption in current cosmological framework, e.g. FLRW, Friedmann world models, etc.

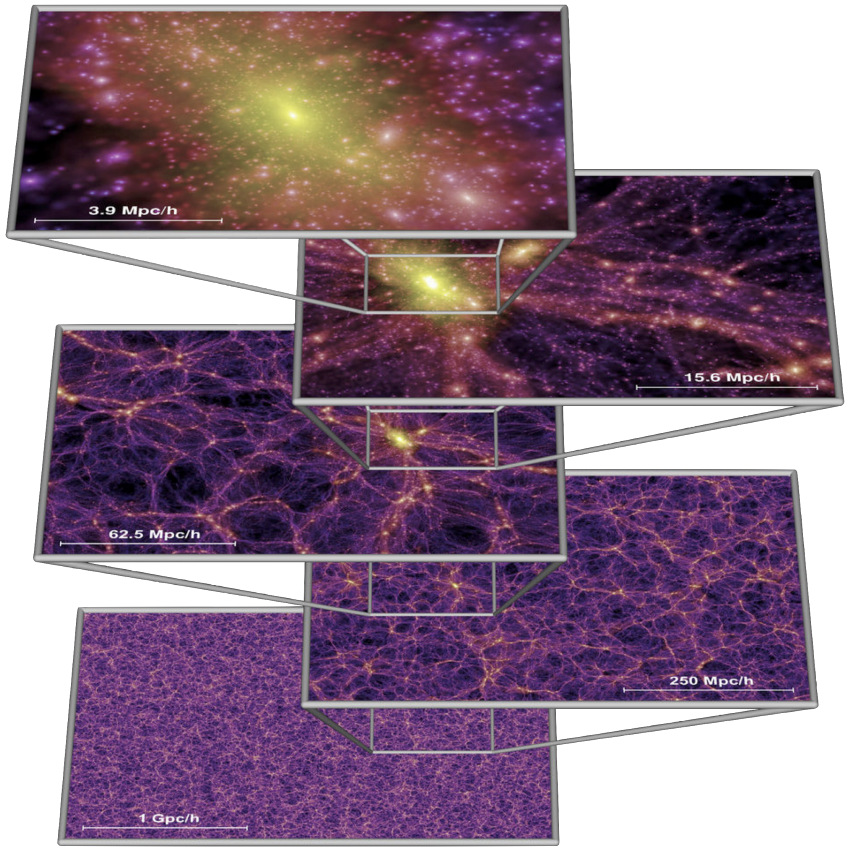

Figure 1: Millennium dark matter simulation (Springel et al., 2005).

$$ds^2 = -c^2 dt^2 + a^2(t)\left[\frac{dr^2}{1-\kappa r^2} + r^2(d\theta^2 + \sin^2\theta d\phi^2)\right]$$

The Cosmic Microwave Background

- The CMB is remarkably smooth ($\Delta T/T \approx 10^{-5}$).

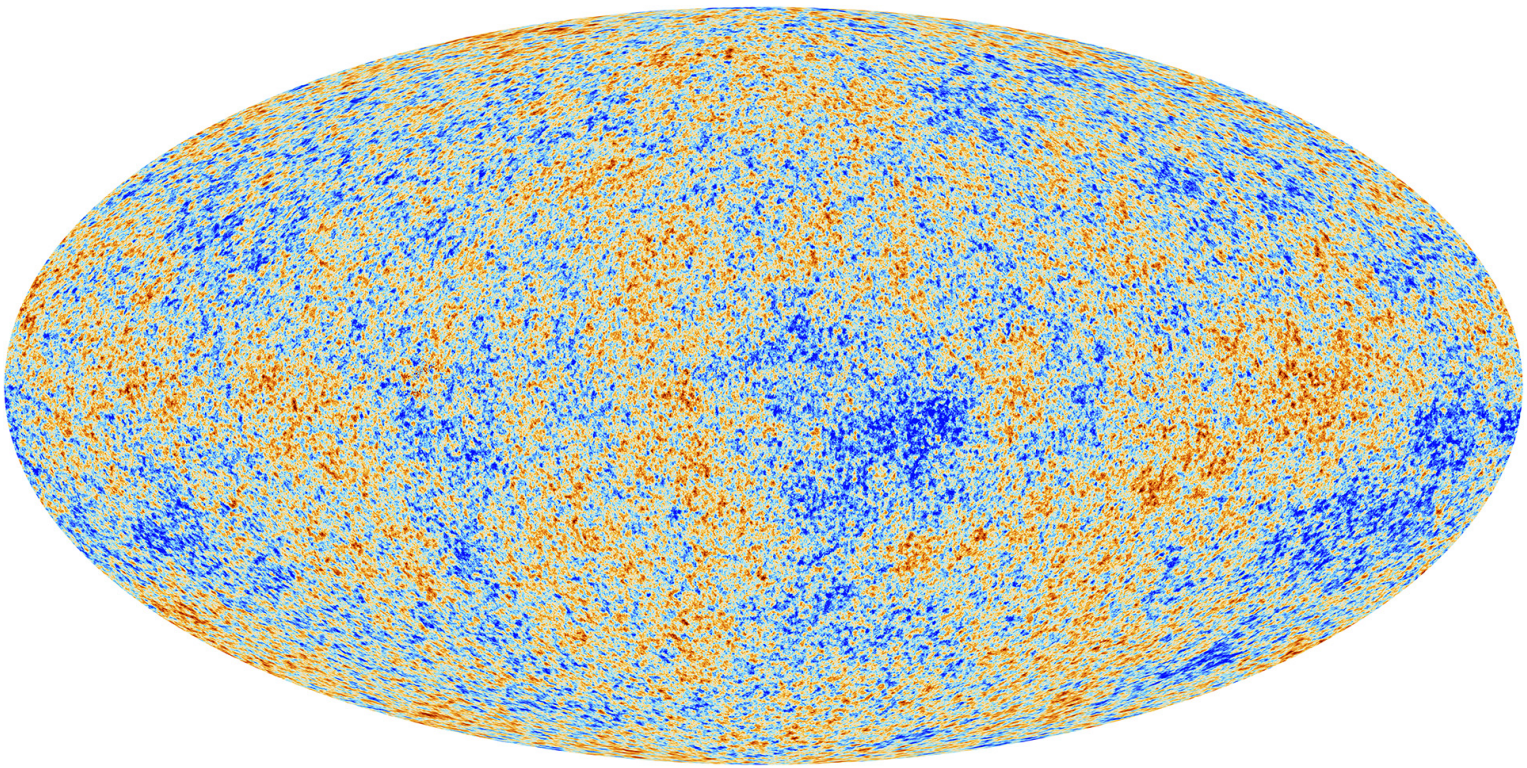

Figure 2: CMB temp. map (dipole subtracted; Planck Collaboration et al., 2020).

The Cosmic Microwave Background

- The CMB is remarkably smooth ($\Delta T/T \approx 10^{-5}$).
- But we see a dipole first ($\Delta T/T \approx 10^{-3}$).

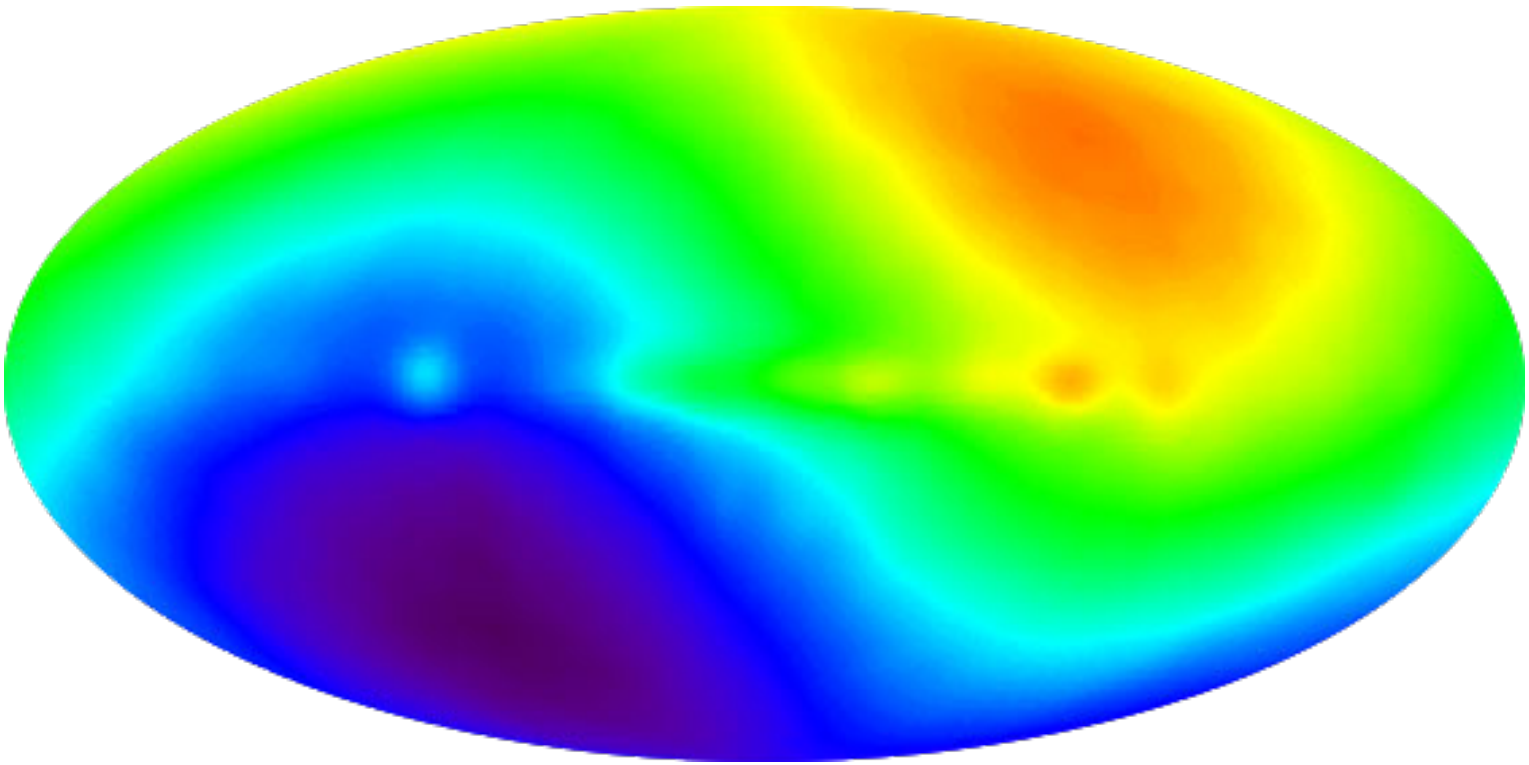

Figure 2: CMB temperature map (dipole included; COBE). ★: dipole direction.

The Cosmic Microwave Background

- The CMB is remarkably smooth ($\Delta T/T \approx 10^{-5}$).
- But we see a dipole first ($\Delta T/T \approx 10^{-3}$).

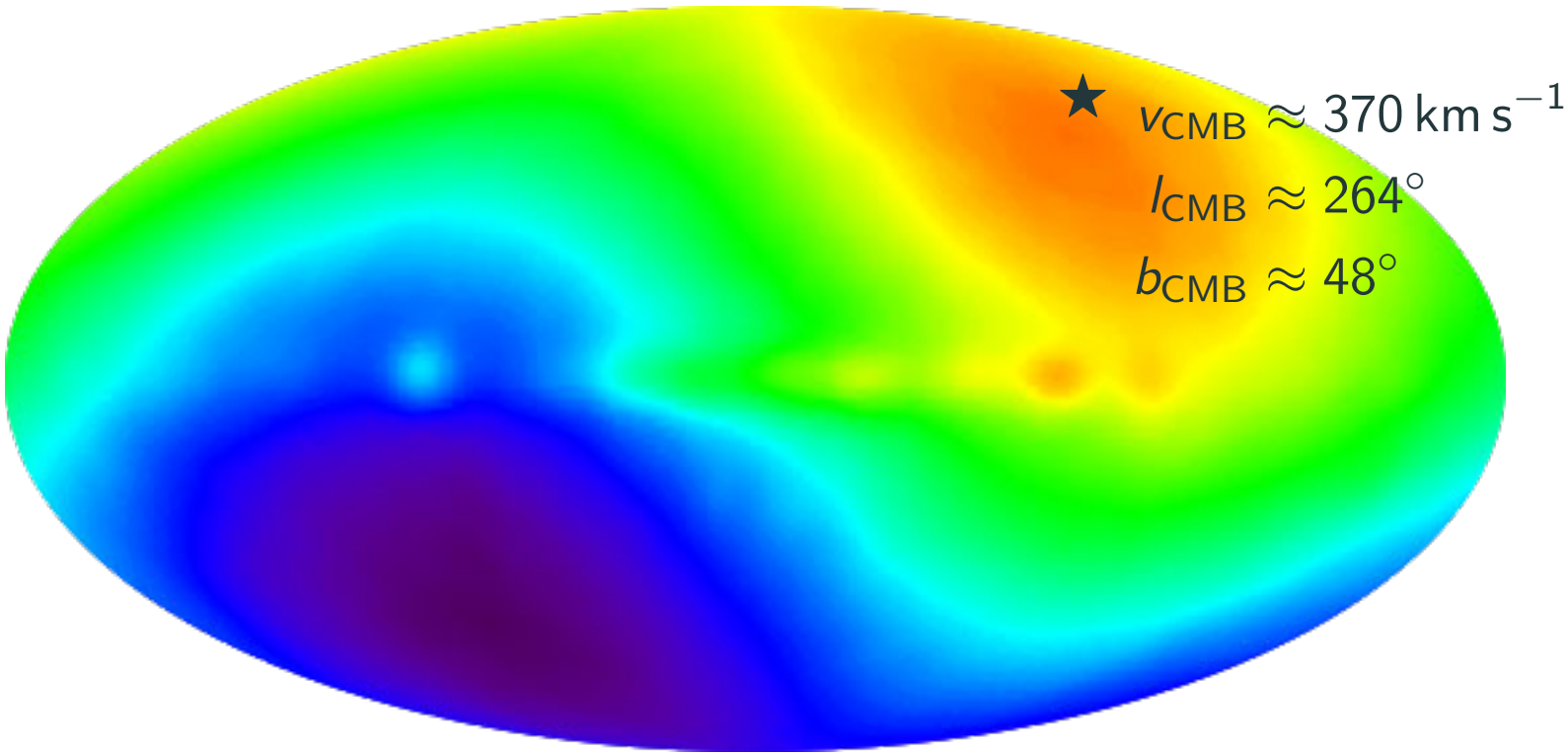

Figure 2: CMB temperature map (dipole included; COBE). ★: dipole direction.

The CMB Dipole

- The CMB dipole ★ is a consequence of our **motion through the Universe** ($v_{CMB} \approx 370$ km s^{-1}).

The CMB Dipole

- The CMB dipole ★ is a consequence of our **motion through the Universe** ($v_{CMB} \approx 370$ km s^{-1}).
- CP $\rightarrow$ the dipole-removed frame is the frame of cosmic rest.

The CMB Dipole

- The CMB dipole ★ is a consequence of our **motion through the Universe** ($v_{CMB} \approx 370$ km s^{-1}).
- CP $\rightarrow$ the dipole-removed frame is the frame of cosmic rest.
- *How do we test the CP?*

The Ellis & Baldwin (1984) Test

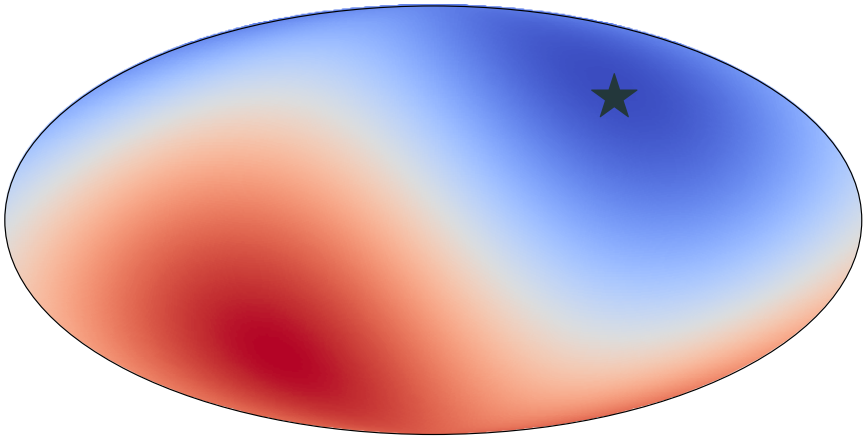

Figure 3: Dipole signal, Doppler shift.

The Ellis & Baldwin (1984) Test

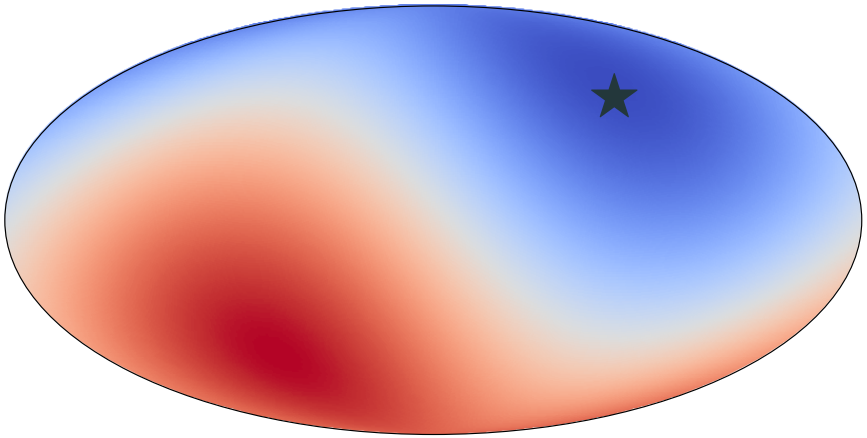

Figure 3: Dipole signal, Doppler shift.

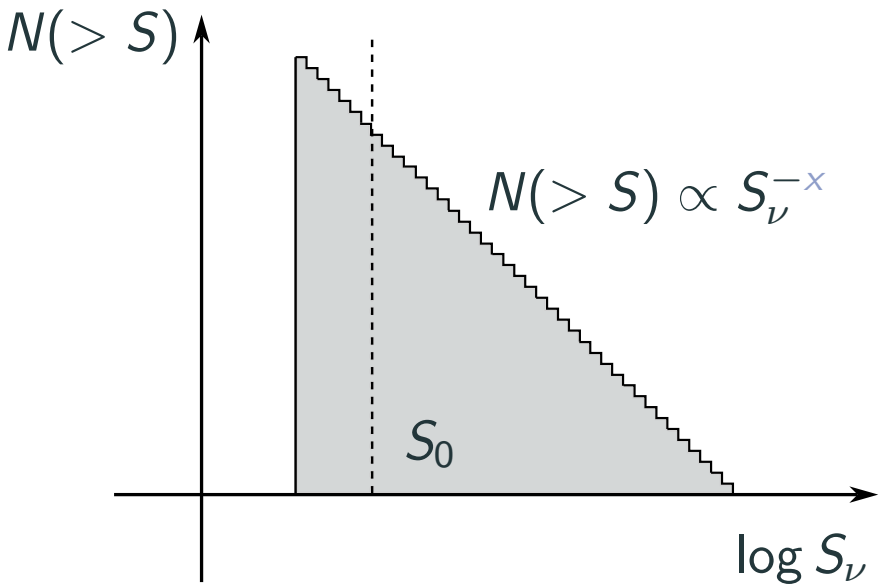

Figure 4: Number of sources above limit S.

The Ellis & Baldwin (1984) Test

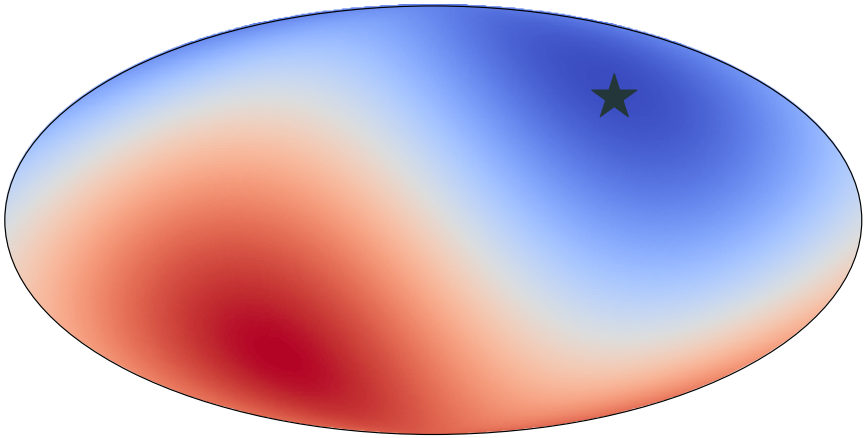

Figure 3: Dipole signal, Doppler shift.

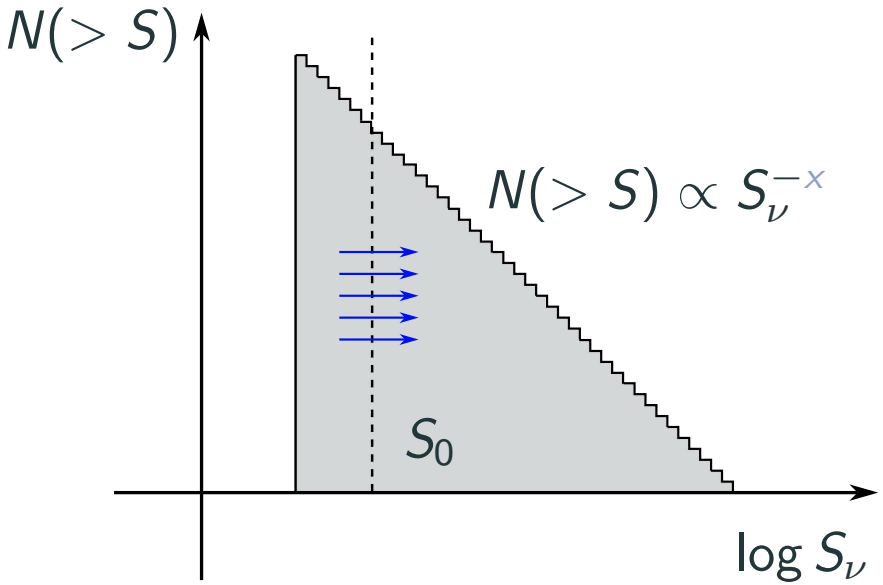

Figure 4: Number of sources above limit S.

The Ellis & Baldwin (1984) Test

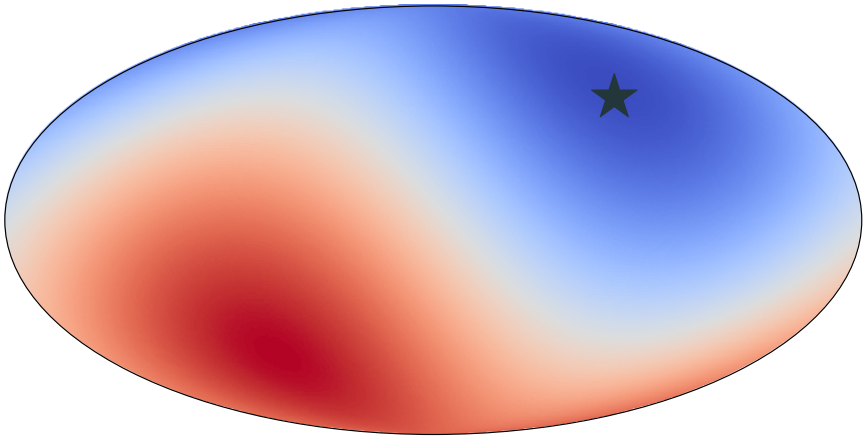

Figure 3: Dipole signal, Doppler shift.

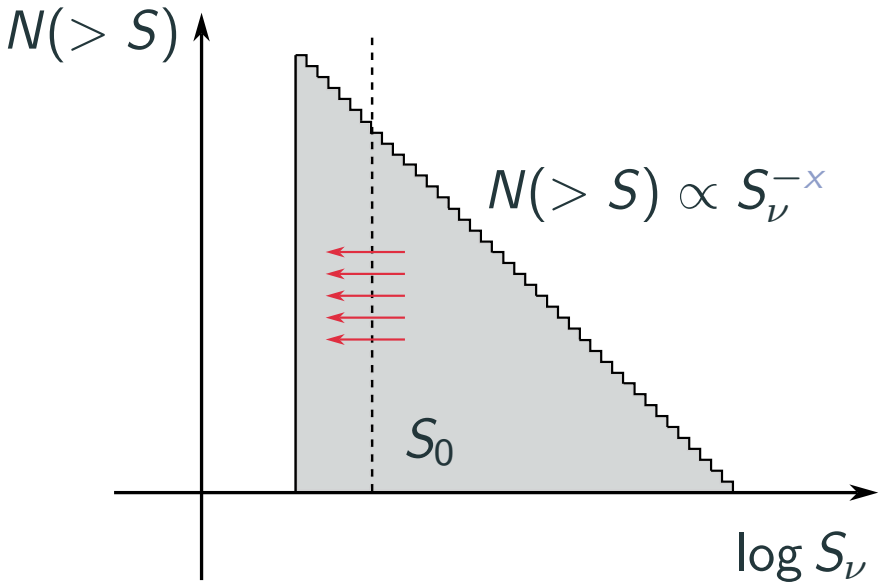

Figure 4: Number of sources above limit S.

The Ellis & Baldwin (1984) Test

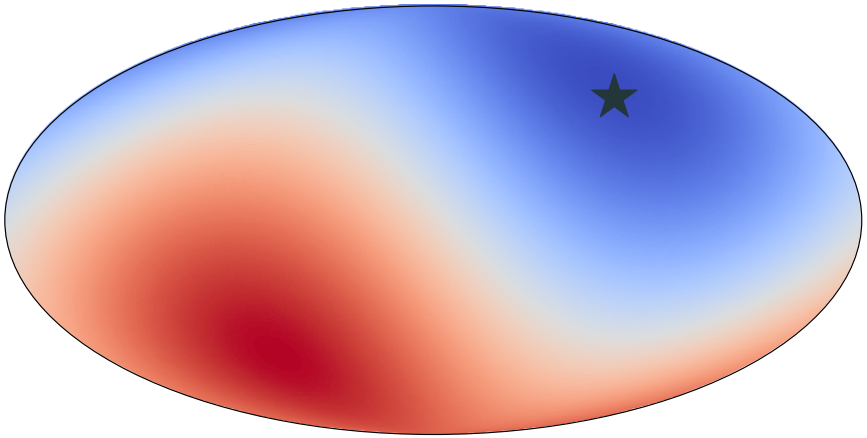

Figure 3: Dipole signal, Doppler shift.

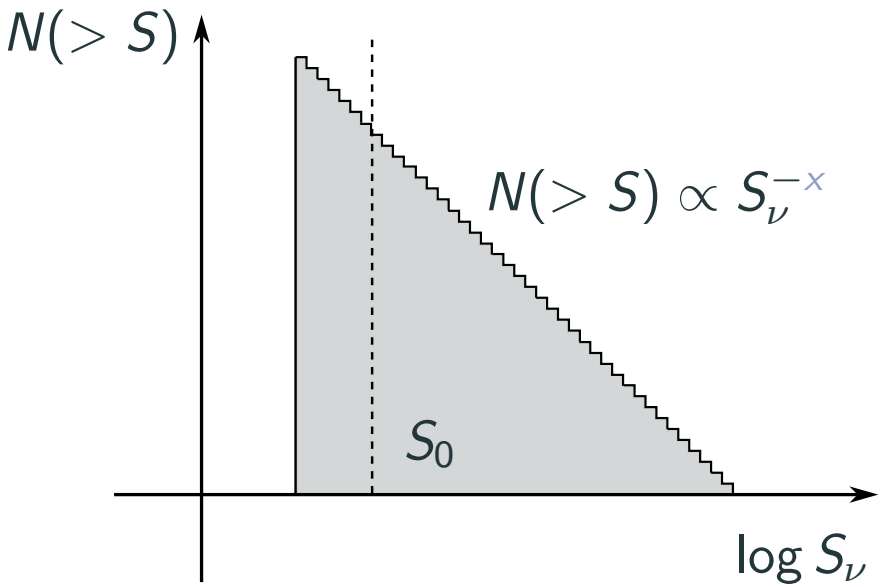

Figure 4: Number of sources above limit S.

The Ellis & Baldwin (1984) Test

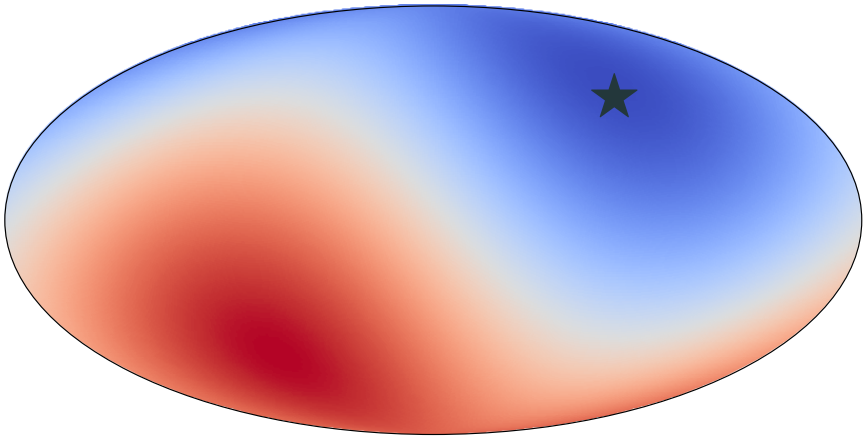

Figure 3: Dipole signal, Doppler shift.

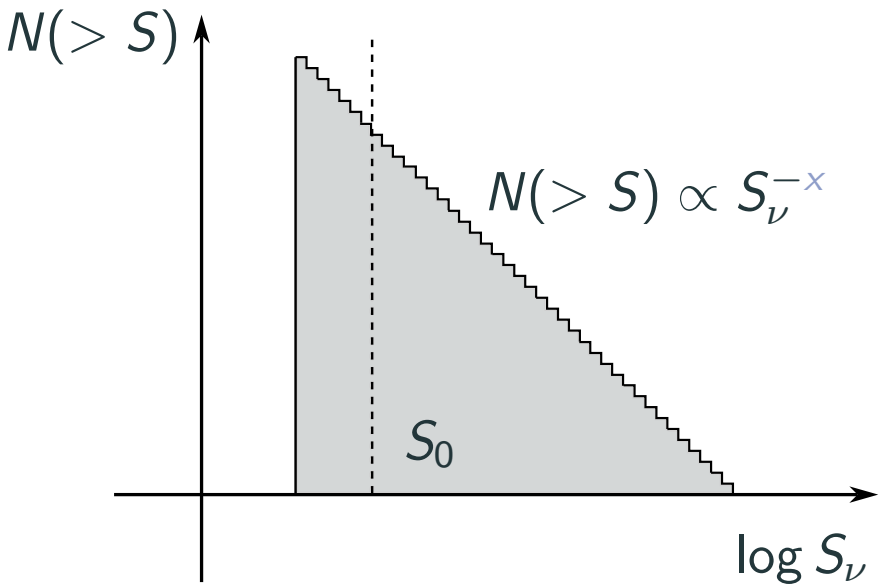

Figure 4: Number of sources above limit S.

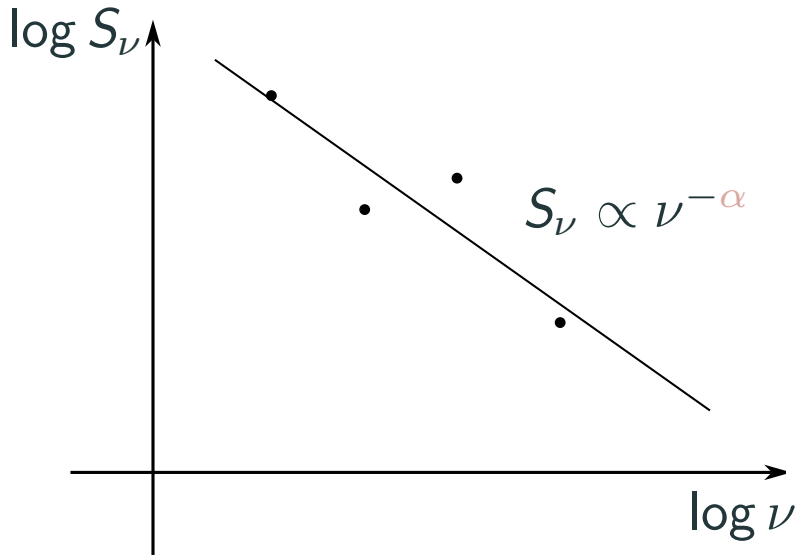

Figure 5: Power law dependence of flux S_ν on frequency ν.

The Ellis & Baldwin (1984) Test

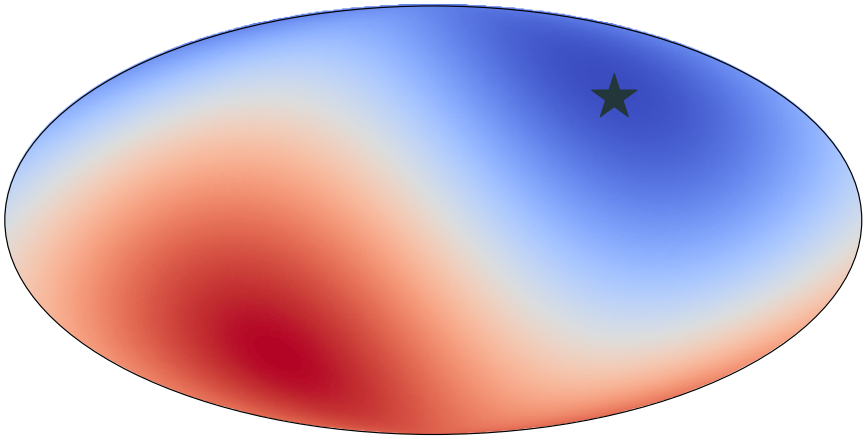

Figure 3: Dipole signal, Doppler shift.

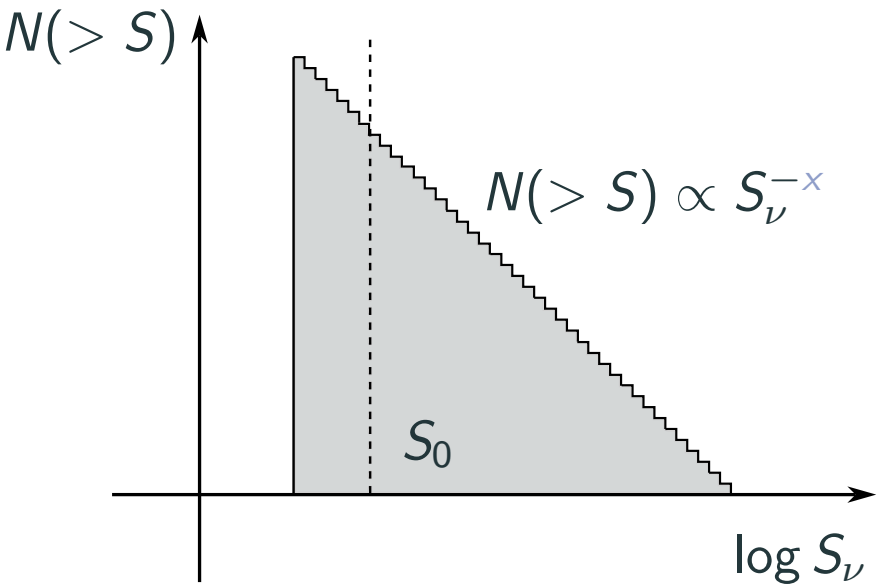

Figure 4: Number of sources above limit S.

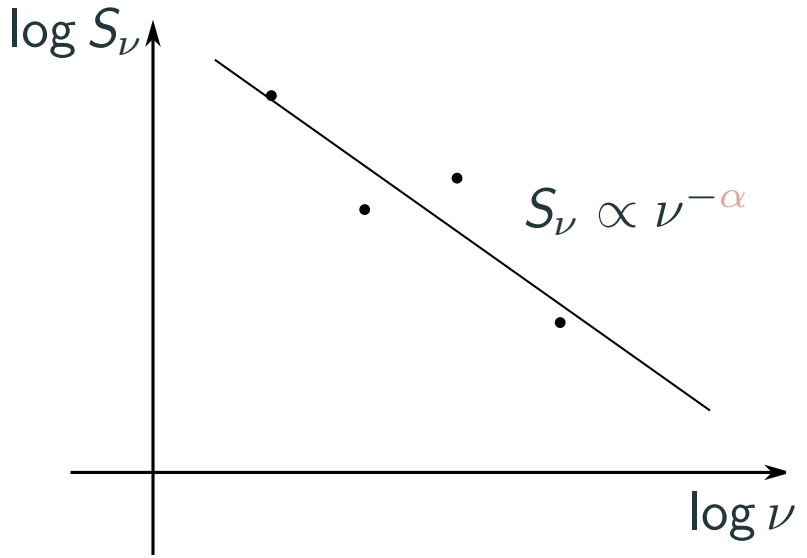

Figure 5: Power law dependence of flux S_ν on frequency ν.

We use only **special relativity** to derive how our peculiar motion impacts observables — like galaxy surveys.

E&B Relation

We use only a handful of relations $\triangleright$ from SR and assumptions $*$ about the source population. Primed variables are our frame.

- $\triangleright$ We know $\nu' = \nu\delta$ — Doppler shift

E&B Relation

We use only a handful of relations $\triangleright$ from SR and assumptions $*$ about the source population. Primed variables are our frame.

- $\triangleright$ We know $\nu' = \nu\delta$ — Doppler shift
- $*$ We assume that sources follow $S_\nu \propto \nu^{-\alpha}$

E&B Relation

We use only a handful of relations $\triangleright$ from SR and assumptions $*$ about the source population. Primed variables are our frame.

- $\triangleright$ We know $\nu' = \nu\delta$ — Doppler shift
- $*$ We assume that sources follow $S_\nu \propto \nu^{-\alpha}$
- $*$ We assume $N(> S) \propto S_\nu^{-x}$

E&B Relation

We use only a handful of relations $\triangleright$ from SR and assumptions $*$ about the source population. Primed variables are our frame.

- $\triangleright$ We know $\nu' = \nu\delta$ — Doppler shift
- $*$ We assume that sources follow $S_\nu \propto \nu^{-\alpha}$
- $*$ We assume $N(> S) \propto S_\nu^{-x}$
- $\triangleright$ We know $d\Omega' = d\Omega\delta^{-2}$ — relativistic aberration

E&B Relation

We use only a handful of relations $\triangleright$ from SR and assumptions $*$ about the source population. Primed variables are our frame.

- $\triangleright$ We know $\nu' = \nu\delta$ — Doppler shift
- $*$ We assume that sources follow $S_\nu \propto \nu^{-\alpha}$
- $*$ We assume $N(>S) \propto S_\nu^{-x}$
- $\triangleright$ We know $d\Omega' = d\Omega\delta^{-2}$ — relativistic aberration

We find a dipolar modulation in source density where

$$\boxed{\mathcal{D} = [2 + x(1 + \alpha)]\,\beta.}$$

E&B Relation

We use only a handful of relations $\triangleright$ from SR and assumptions $*$ about the source population. Primed variables are our frame.

- $\triangleright$ We know $\nu' = \nu\delta$ — Doppler shift
- $*$ We assume that sources follow $S_\nu \propto \nu^{-\alpha}$
- $*$ We assume $N(>S) \propto S_\nu^{-x}$
- $\triangleright$ We know $d\Omega' = d\Omega\delta^{-2}$ — relativistic aberration

We find a dipolar modulation in source density where

$$\boxed{\mathcal{D} = [2 + x(1+\alpha)]\,\beta.}$$

$\alpha = 0.75$, $x = 1$, $\beta = v_{\rm CMB}/c = 0.00123 \implies \mathcal{D} = 0.0046.$

A 0.5% effect!

Measurements of the Cosmic Dipole

$$\mathcal{D}_{\mathrm{CMB}} = \underbrace{[2 + x(1+\alpha)] \times v_{\mathrm{CMB}}/c}_{\text{expectation}} \quad \text{vs.} \quad \underbrace{N_{\mathrm{cell}} = \bar{N}(1 + \mathcal{D}\cos\theta)}_{\text{reality}}$$

Measurements of the Cosmic Dipole

$$\underbrace{\mathcal{D}_{\mathrm{CMB}} = [2 + x(1+\alpha)] \times v_{\mathrm{CMB}}/c}_{\text{expectation}} \quad \text{vs.} \quad \underbrace{N_{\mathrm{cell}} = \bar{N}(1 + \mathcal{D}\cos\theta)}_{\text{reality}}$$

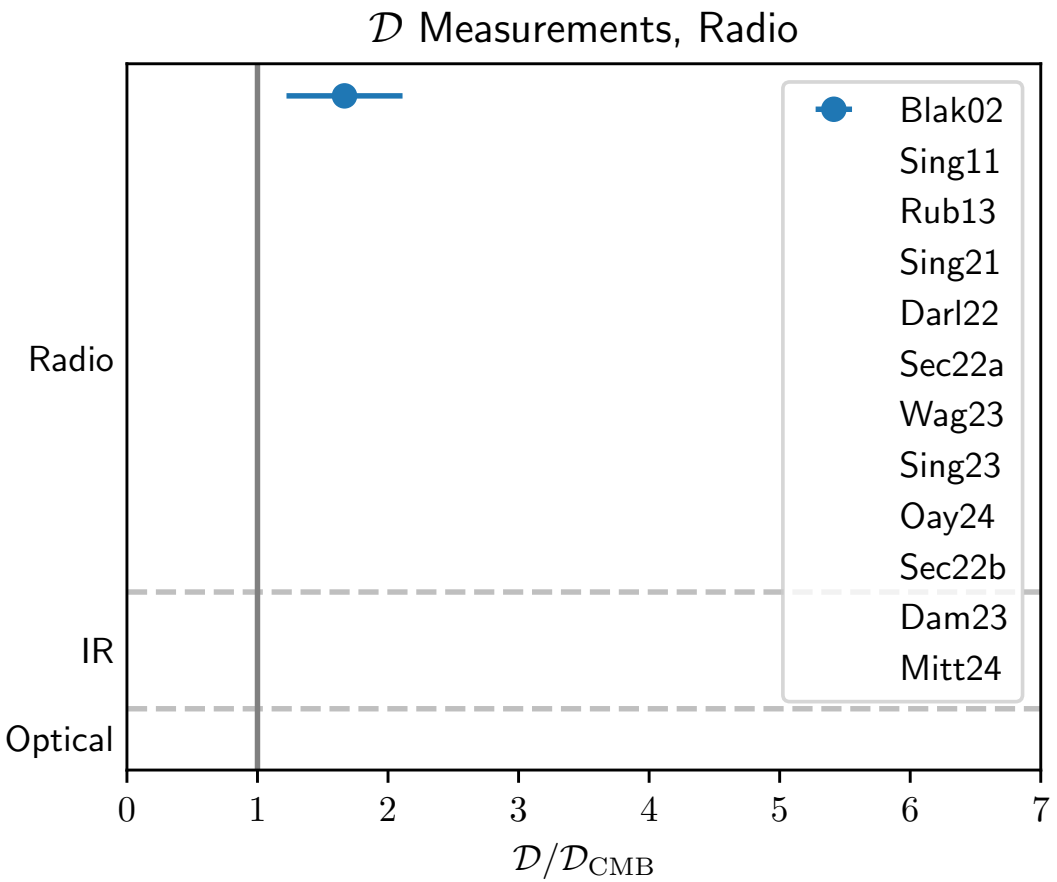

Measurements of the Cosmic Dipole

$$\mathcal{D}_{\rm CMB} = \underbrace{[2 + x(1+\alpha)] \times v_{\rm CMB}/c}_{\text{expectation}} \quad \text{vs.} \quad \underbrace{N_{\rm cell} = \bar{N}(1 + \mathcal{D}\cos\theta)}_{\text{reality}}$$

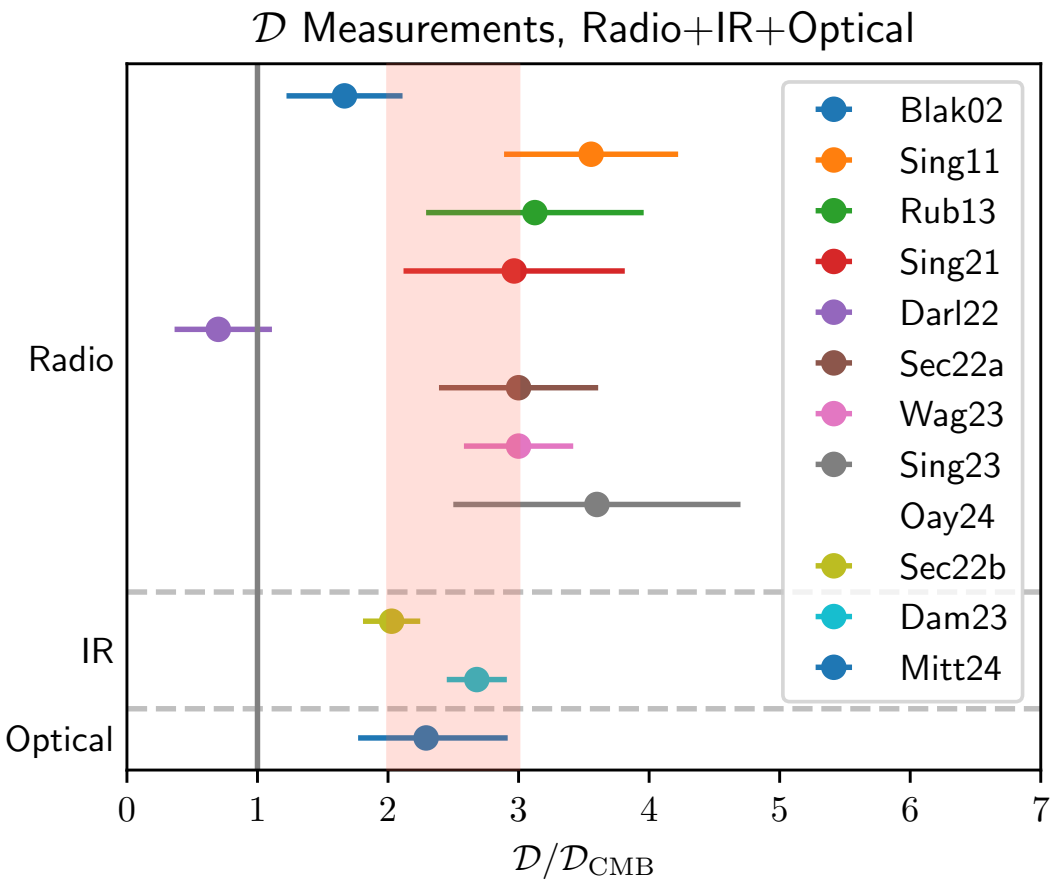

Figure 6: Literature values for $\mathcal{D}$ across radio, optical and near-IR samples (1σ uncertainties). Key samples: **NVSS**, **RACS-low**, **CatWISE2020**, **Quaia**.

Results of Secrest et al. (2021) — IR

Amplitude $\approx \times 2$ larger than CMB expectation at significance of 5σ.

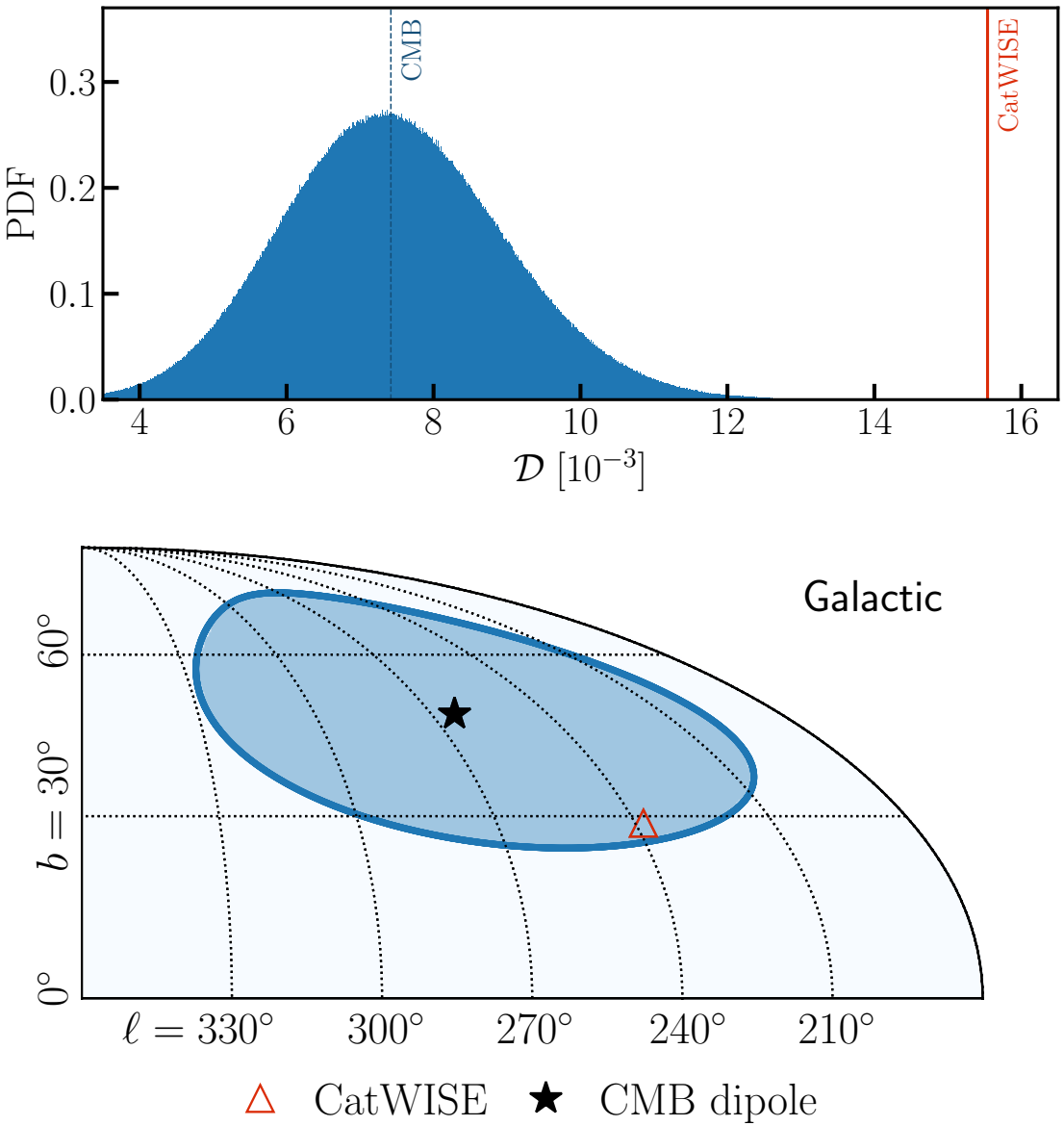

Confirmed by Dam et al. (2023) with a Bayesian approach.

Figure 7: Results from Secrest et al. (2021). *Top:* Statistical significance (5σ) of the CatWISE dipole amplitude. *Bottom*: Significance of the direction of the dipole in CatWISE (2σ contour).

Results of Mittal, Oayda & Lewis (2024) — Optical

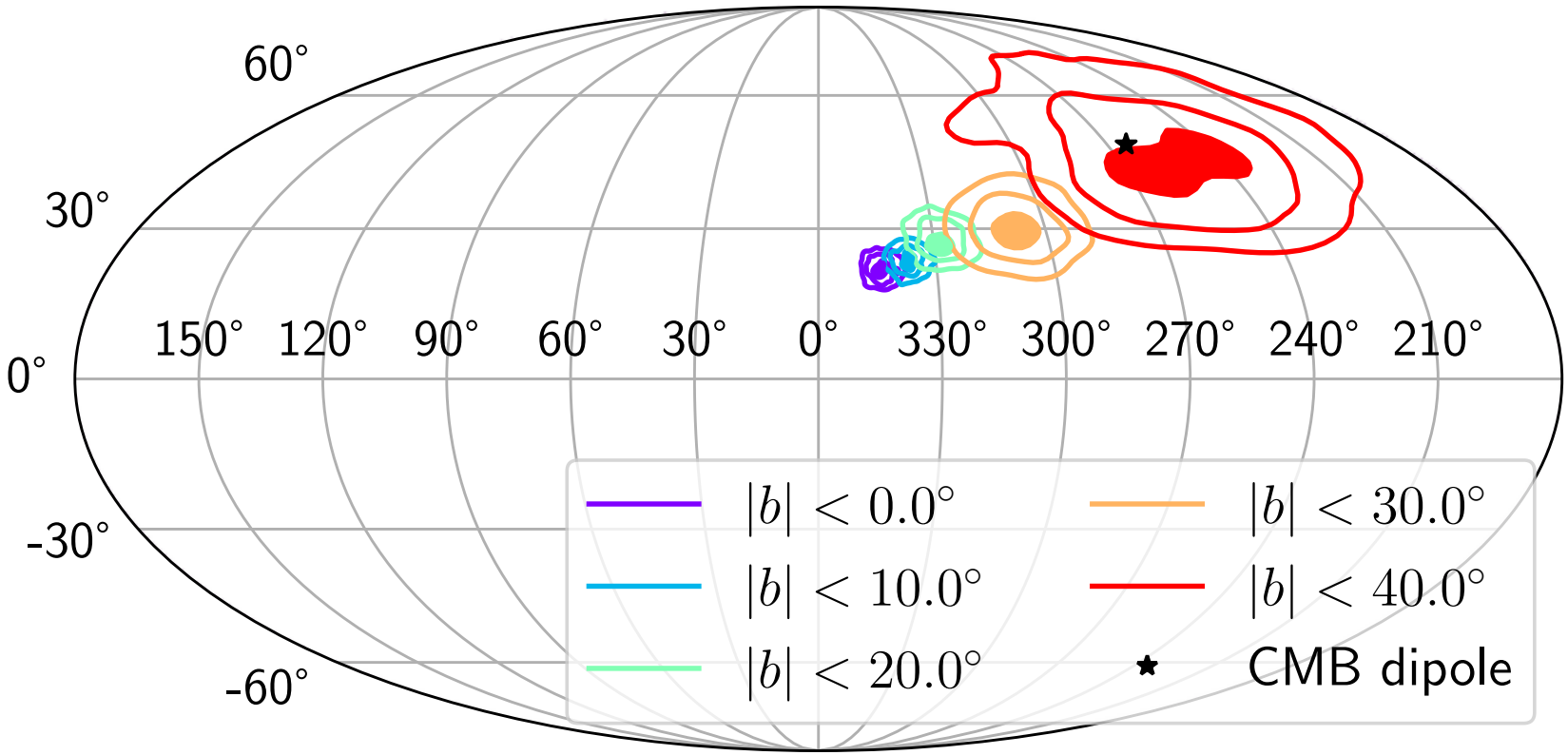

Amplitude D (10^{-3})	37^{+4}_{-4}	34^{+4}_{-4}	25^{+5}_{-5}	17^{+6}_{-6}	11^{+6}_{-5}	5★

Figure 8: Results from Quaia low ($G < 20.0$) as in Mittal et al. (2024). *Top:* projection of marginal posterior for dipole direction onto the sky. *Bottom:* 2σ credible interval for dipole amplitude by mask choice.

Results of Wagenveld et al. (2023) — Radio

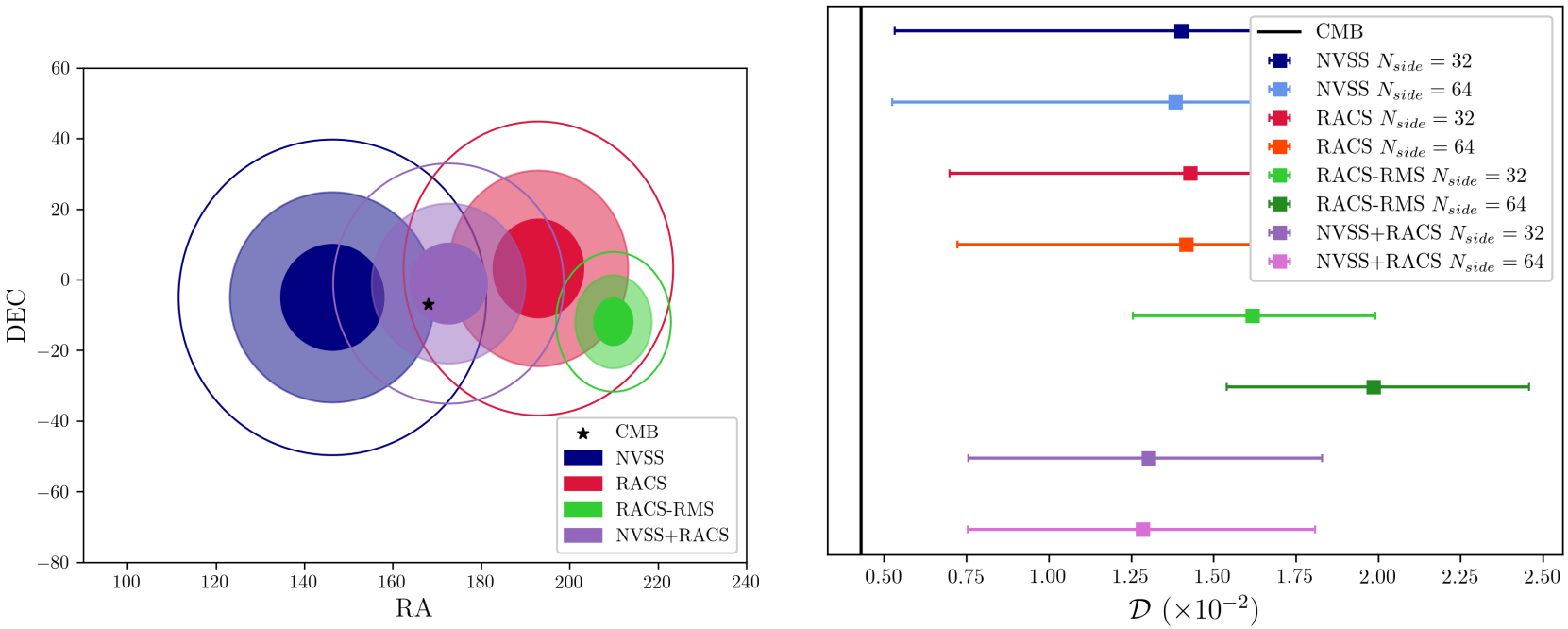

Figure 9: Results of Wagenveld et al. (2023) also point towards an excessive dipole amplitude (but consistent direction).

- '**W23**' — used as prior likelihood later.
- We also analysed NVSS and RACS-low, but with a different approach.

Why is the dipole amplitude larger than expected?

Analysis

Samples We Tested

NVSS (NRAO VLA Sky Survey): 1993–97, 1.4 GHz, northern sky.

RACS-low (Rapid Australian SKA Pathfinder Continuum Survey): 2019–20, 887.5 MHz, southern sky.

Figure 10: *Top:* VLA in New Mexico (credit: NRAO). *Bottom:* Australian SKA Pathfinder in Western Australia (credit: CSIRO).

Some Systematic Effects

Some issues to mitigate:

Some Systematic Effects

Some issues to mitigate:

- Catalogue completeness at a given S_ν.

Some Systematic Effects

Some issues to mitigate:

- Catalogue completeness at a given S_ν.
- Declination-dependent systematics.

Some Systematic Effects

Some issues to mitigate:

- Catalogue completeness at a given S_ν.
- Declination-dependent systematics.
- Contamination from the Galactic plane and bright radio sources.

Preparing NVSS & RACS

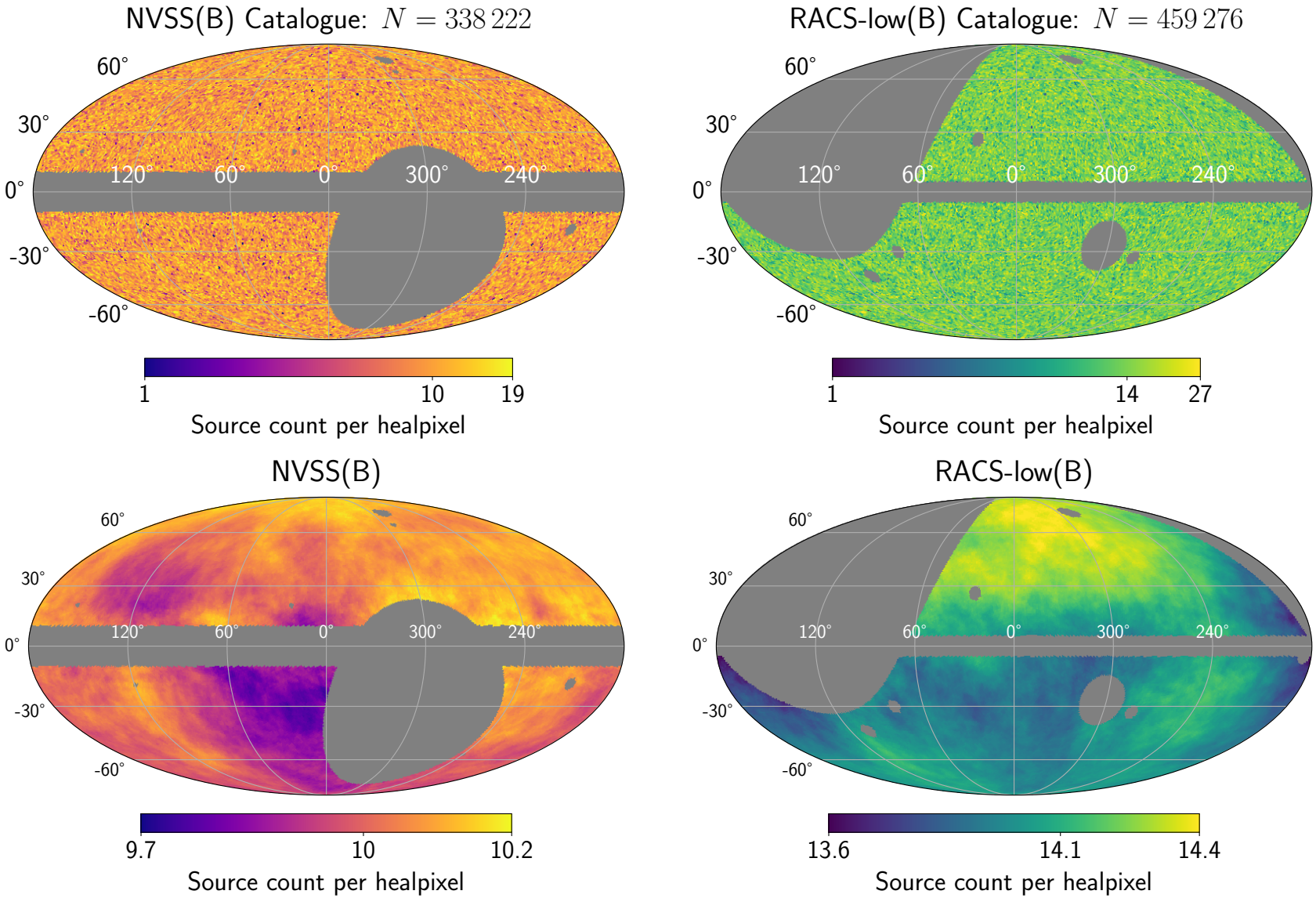

Figure 11: NVSS and RACS-low samples in Galactic coordinates binned into healpixels. *Top:* Raw density maps. *Bottom:* Smoothed density maps.

Cross-matching Local Sources

Remove **nearby structure**, which complicates the picture.

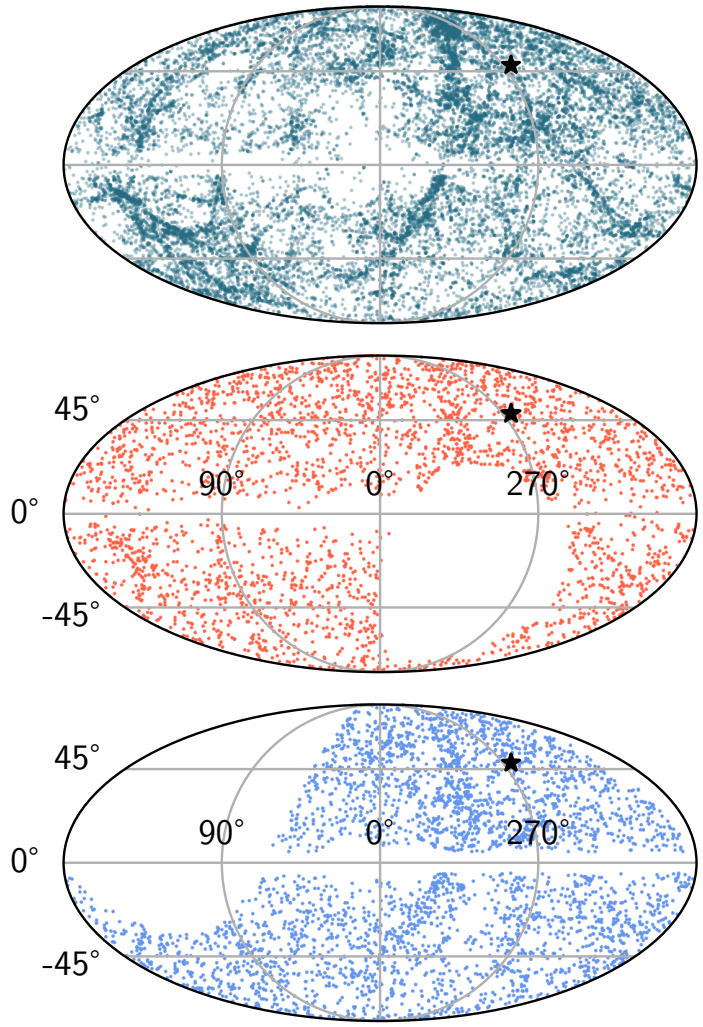

Figure 12: *Top:* 2MRS, $z < 0.02$. *Middle:* NVSS. *Bottom:* RACS-low.

Cross-matching Local Sources

Remove **nearby structure**, which complicates the picture.

Cross-match NVSS and RACS-low radio sources with counterparts: **2MRS** (near-IR); **NED** (radio).

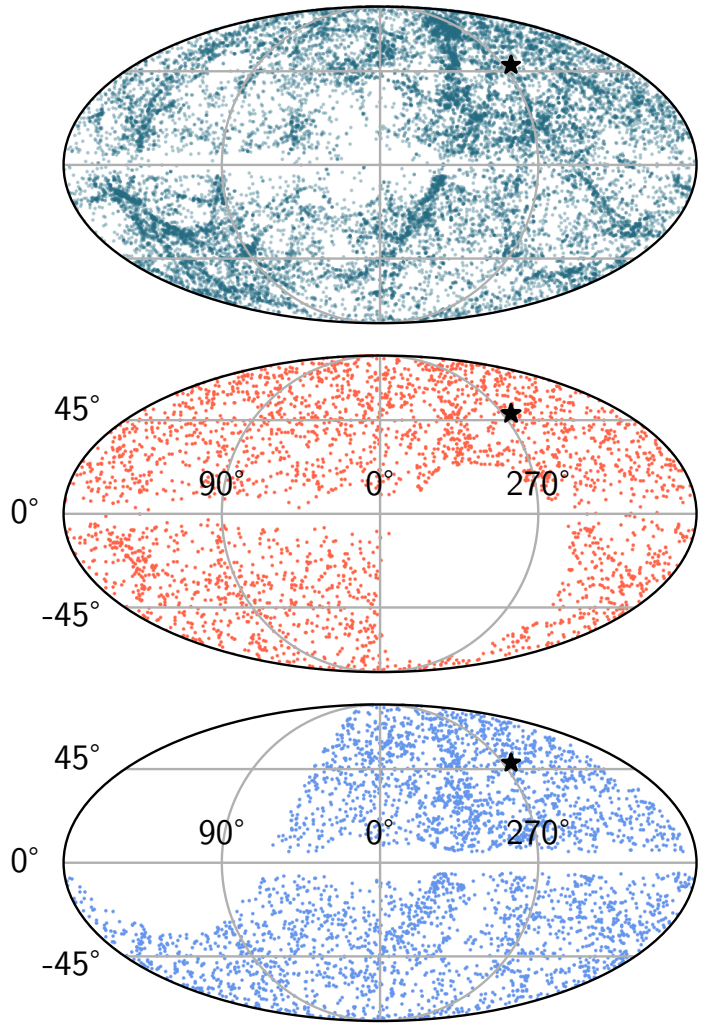

Figure 12: *Top:* 2MRS, $z < 0.02$. *Middle:* NVSS. *Bottom:* RACS-low.

Statistics: Bayesian Inference

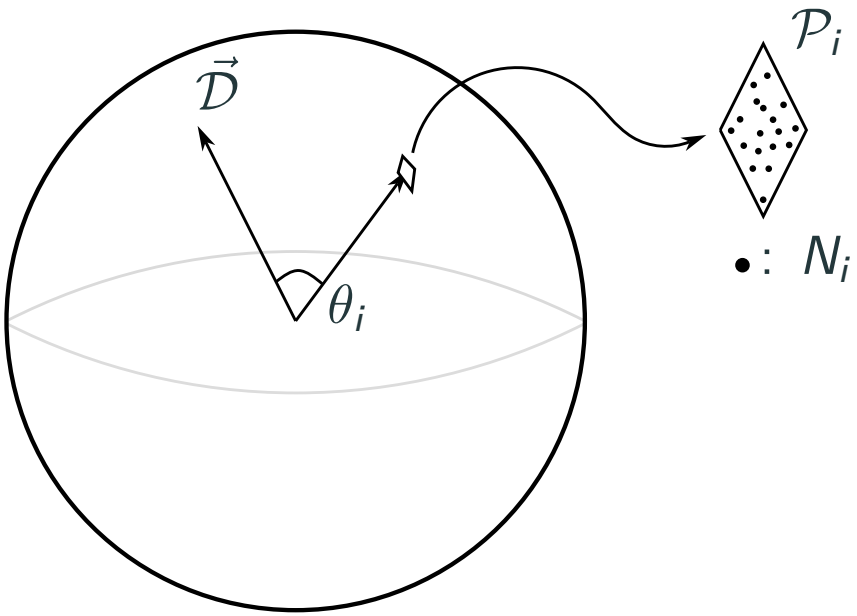

Figure 13: Schematic of pixel $\mathcal{P}_i$ on the celestial sphere with N_i sources $(\cdot)$ near dipole vector $\vec{\mathcal{D}}$.

Dipole vector $\vec{\mathcal{D}}$ is a free parameter.

Statistics: Bayesian Inference

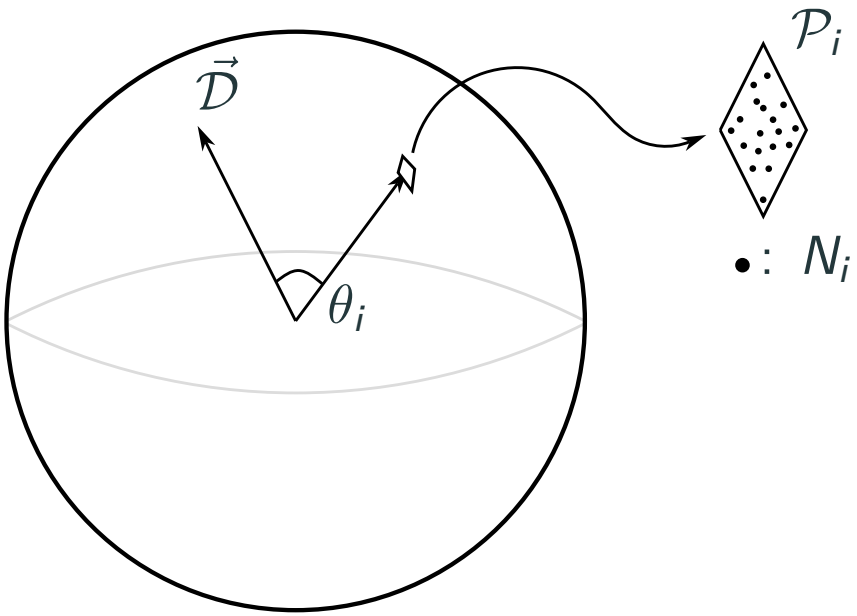

Figure 13: Schematic of pixel $\mathcal{P}_i$ on the celestial sphere with N_i sources $(\cdot)$ near dipole vector $\vec{\mathcal{D}}$.

Dipole vector $\vec{\mathcal{D}}$ is a free parameter.

- Pixel $\mathcal{P}_i$ has N_i sources.

Statistics: Bayesian Inference

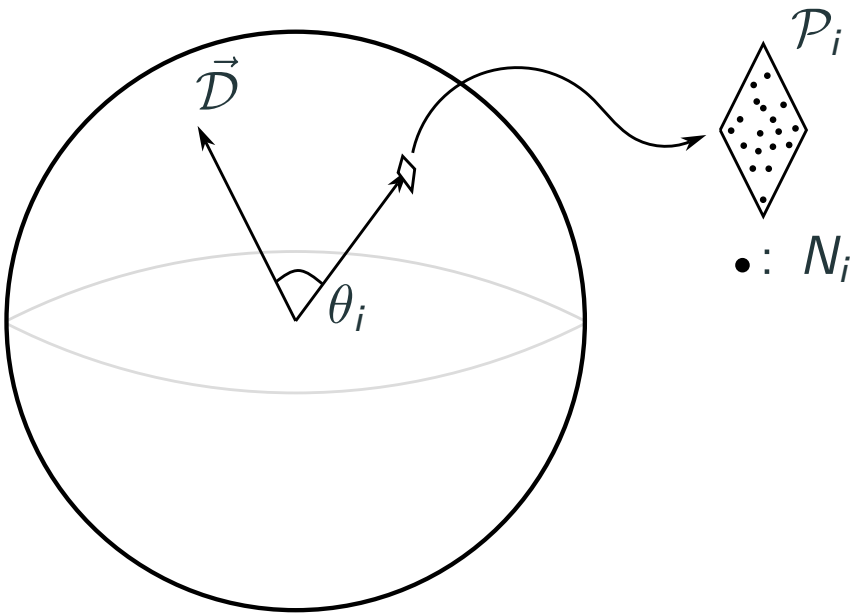

Figure 13: Schematic of pixel $\mathcal{P}_i$ on the celestial sphere with N_i sources $(\cdot)$ near dipole vector $\vec{\mathcal{D}}$.

Dipole vector $\vec{\mathcal{D}}$ is a free parameter.

- Pixel $\mathcal{P}_i$ has N_i sources.
- $\mathbb{E}[N_i] = \bar{N}(1 + \mathcal{D}\cos\theta_i)$

Statistics: Bayesian Inference

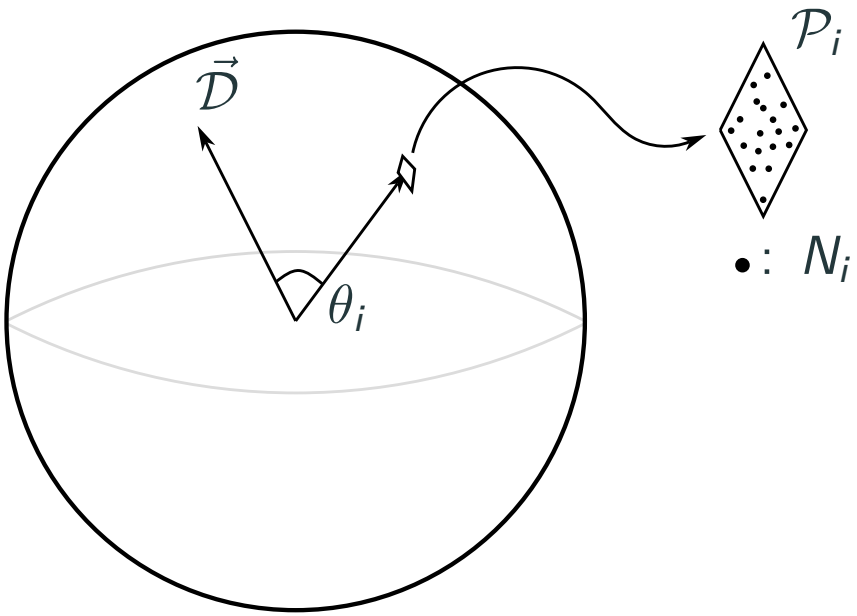

Figure 13: Schematic of pixel $\mathcal{P}_i$ on the celestial sphere with N_i sources $(\cdot)$ near dipole vector $\vec{\mathcal{D}}$.

Dipole vector $\vec{\mathcal{D}}$ is a free parameter.

- Pixel $\mathcal{P}_i$ has N_i sources.
- $\mathbb{E}[N_i] = \bar{N}(1 + \mathcal{D}\cos\theta_i)$
- Construct a probability map over the sky.

Statistics: Bayesian Inference

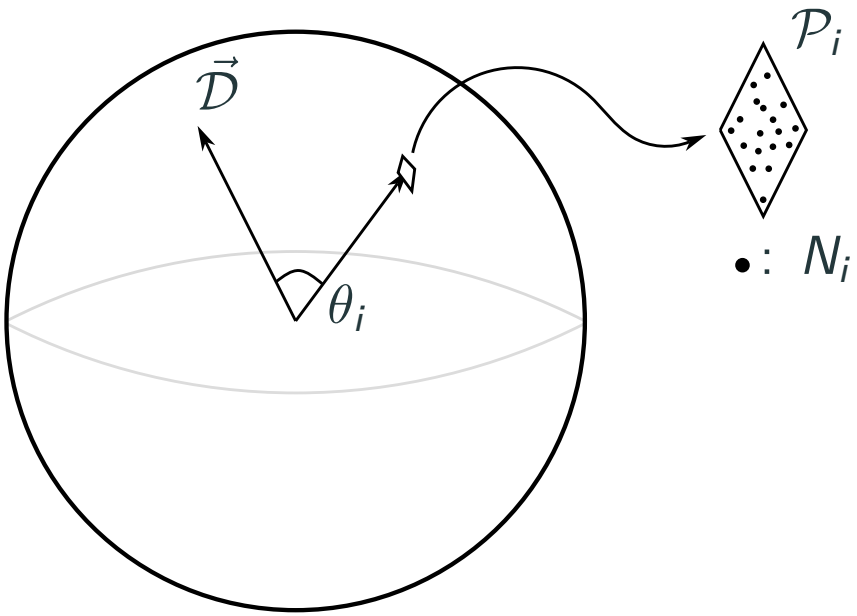

Figure 13: Schematic of pixel $\mathcal{P}_i$ on the celestial sphere with N_i sources $(\cdot)$ near dipole vector $\vec{\mathcal{D}}$.

Dipole vector $\vec{\mathcal{D}}$ is a free parameter.

- Pixel $\mathcal{P}_i$ has N_i sources.
- $\mathbb{E}[N_i] = \bar{N}(1 + \mathcal{D}\cos\theta_i)$
- Construct a probability map over the sky.

Yields the likelihood function

$$\ln \mathcal{L} = \sum_{i=1}^{n_{\text{pix.}}} N_i \ln \hat{f}_i.$$

Statistics: Bayesian Inference

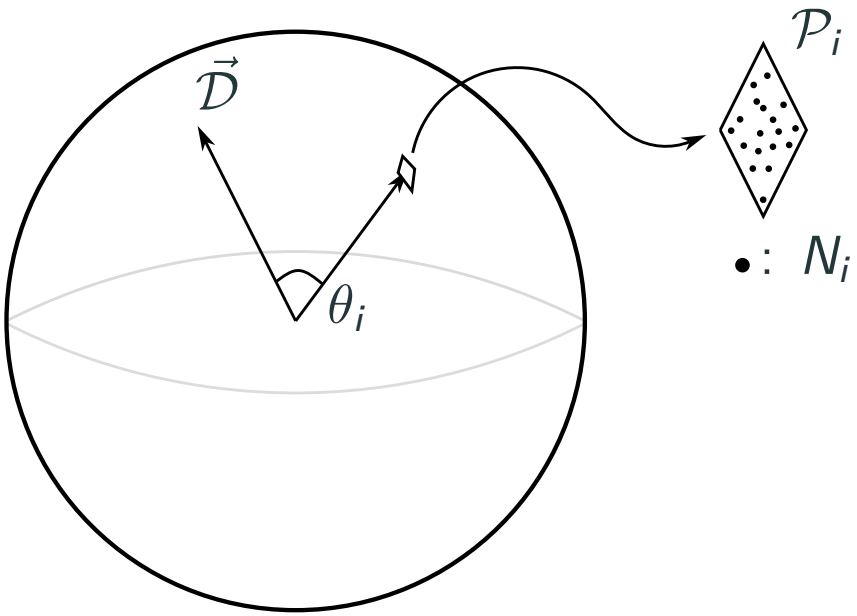

Figure 13: Schematic of pixel $\mathcal{P}_i$ on the celestial sphere with N_i sources $(\cdot)$ near dipole vector $\vec{\mathcal{D}}$.

Dipole vector $\vec{\mathcal{D}}$ is a free parameter.

- Pixel $\mathcal{P}_i$ has N_i sources.
- $\mathbb{E}[N_i] = \bar{N}(1 + \mathcal{D}\cos\theta_i)$
- Construct a probability map over the sky.

Yields the likelihood function

$$\ln \mathcal{L} = \sum_{i=1}^{n_{\text{pix.}}} N_i \ln \hat{f}_i.$$

Use a Bayesian statistical approach to infer posterior probability distribution for $\mathcal{D}$, l and b. Analyse individually and jointly.

Statistics: Second Inference Level

	Short label	Description
M_0	Null	Monopole
M_1	Free dipole	Free $\mathcal{D}$, l, b
M_2	Kinematic velocity	$\mathcal{D}$ fixed and free l, b
M_3	Kinematic direction	l, b fixed and free $\mathcal{D}$
M_4	Kinematic dipole	All parameters fixed to CMB expectation
M_5	W23	$\mathcal{D}$, l, b from Wagenveld et al. (2023)

Table 1: The six models tested and ranked.

Compare models' explanatory power with marginal likelihood $P(\vec{D}|M)$.

Results

NVSS & RACS: Individual Results

$$\boxed{\mathcal{D}_{\mathrm{CMB}} \approx 0.004}$$

NVSS & RACS: Individual Results

$$\mathcal{D}_{\mathrm{CMB}} \approx 0.004$$

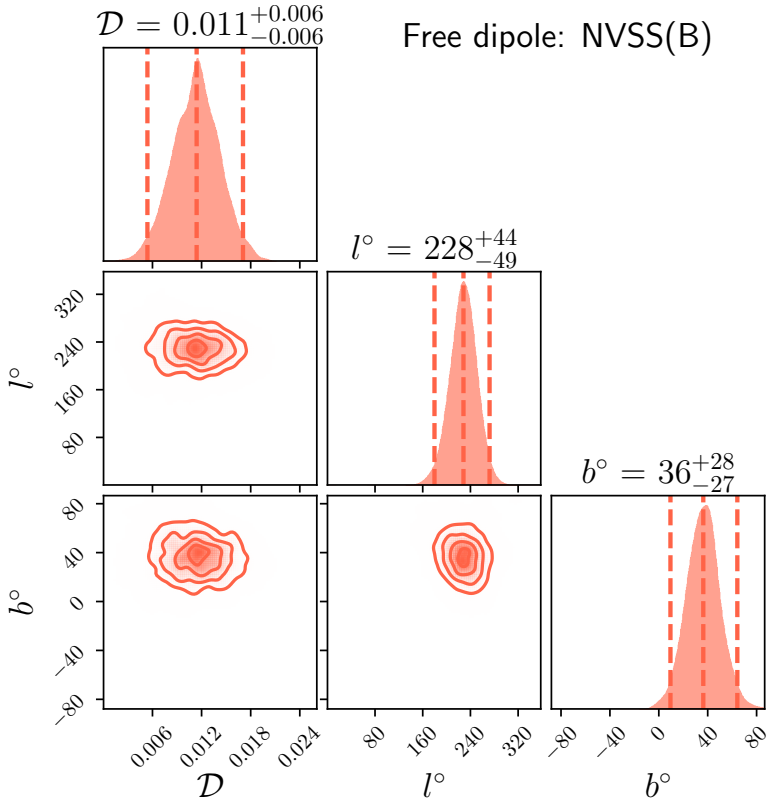

Model		ln B_{i0}
M_1	Free dipole	3.1
M_3	Kin. direction	4.5
M_4	Kin. dipole	4.8

NVSS & RACS: Individual Results

$$\mathcal{D}_{\mathrm{CMB}} \approx 0.004$$

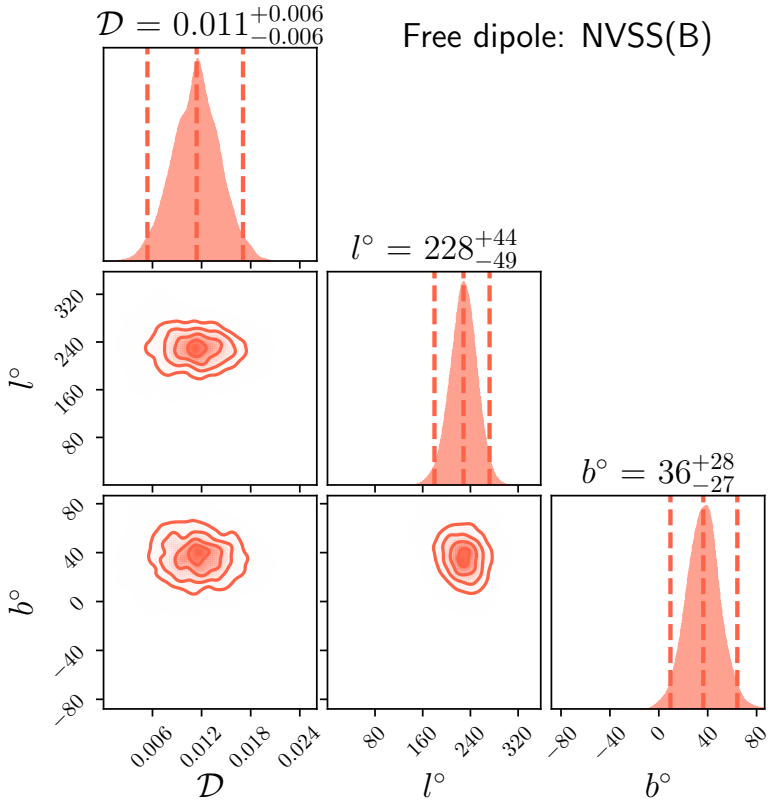

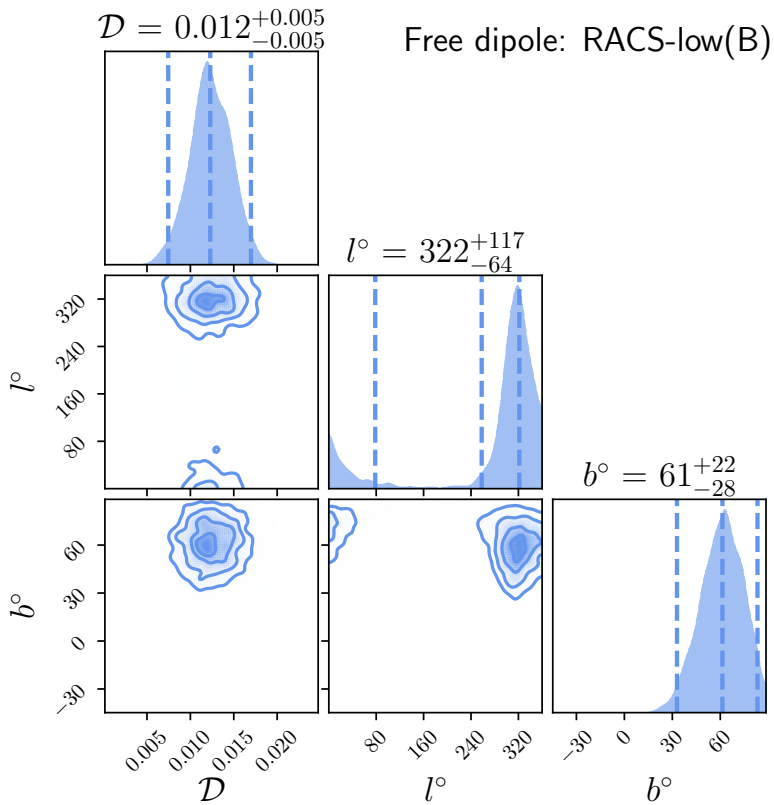

Model		$\ln B_{i0}$
M_1	Free dipole	3.1
M_3	Kin. direction	4.5
M_4	Kin. dipole	4.8

Model		$\ln B_{i0}$
M_1	Free dipole	8.2
M_3	Kin. direction	7.5
M_4	Kin. dipole	6.6

Joint Analysis: NVSS + RACS-low

$$\boxed{\mathcal{D}_{\mathrm{CMB}} \approx 0.004} \quad \text{—} \ln \mathcal{L} = \ln \mathcal{L}_{\mathrm{NVSS}} + \ln \mathcal{L}_{\mathrm{RACS}}$$

Joint Analysis: NVSS + RACS-low

$$\boxed{\mathcal{D}_{\mathrm{CMB}} \approx 0.004} \quad \text{— } \ln \mathcal{L} = \ln \mathcal{L}_{\mathrm{NVSS}} + \ln \mathcal{L}_{\mathrm{RACS}}$$

Free dipole: joint

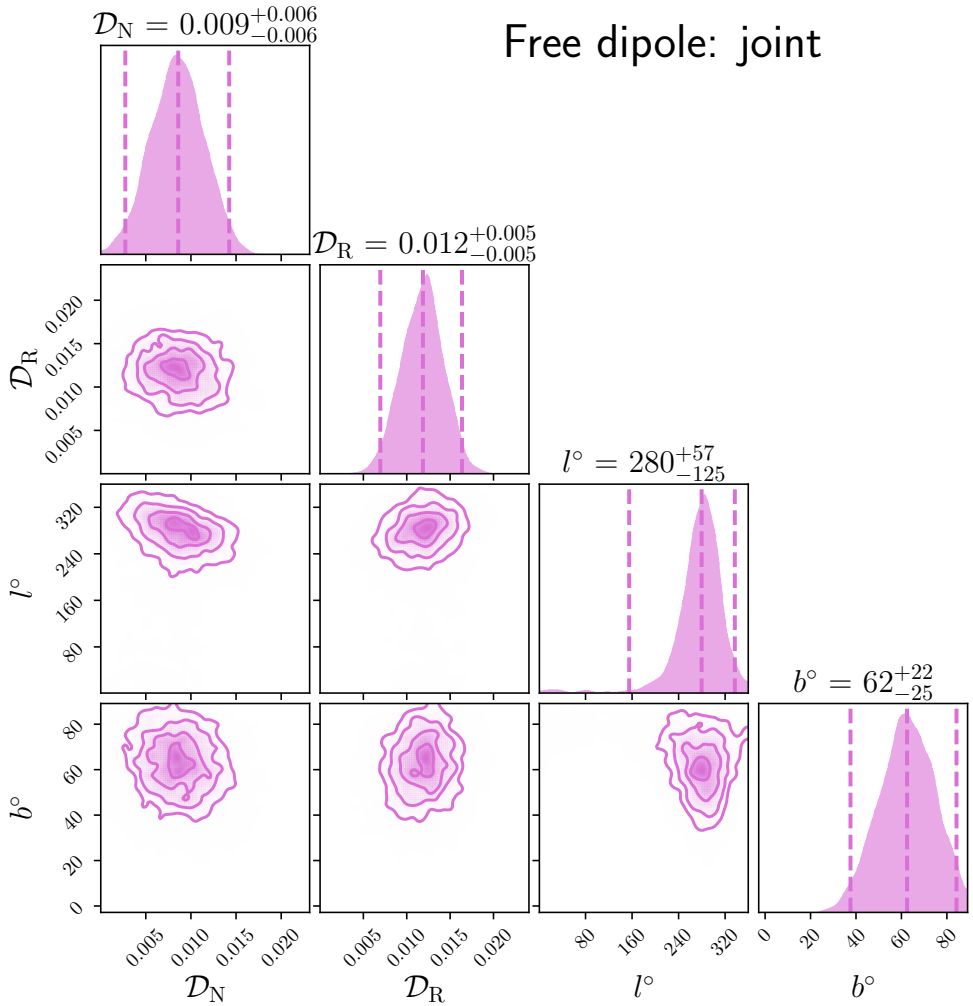

Joint Analysis: NVSS + RACS-low

$$\boxed{\mathcal{D}_{\mathrm{CMB}} \approx 0.004} \quad — \ln \mathcal{L} = \ln \mathcal{L}_{\mathrm{NVSS}} + \ln \mathcal{L}_{\mathrm{RACS}}$$

Free dipole: joint

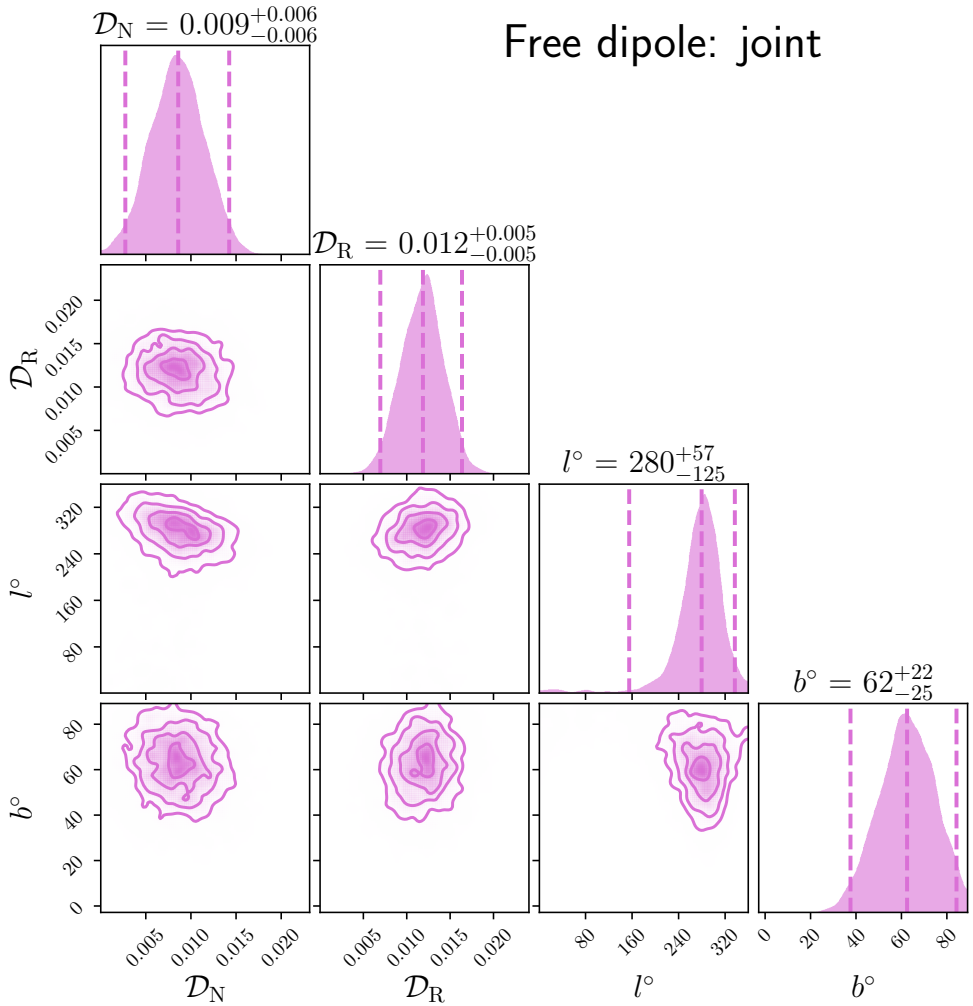

Model		$\ln B_{i0}$
M_3	Kin. dir.	12.1
M_4	Kin. dipole	11.4
M_5	W23	17.1

M_3 (kinematic direction):

$\mathcal{D}_{\mathrm{NVSS}} \approx (10 \pm 5) \times 10^{-3}$

$\mathcal{D}_{\mathrm{RACS}} \approx (11 \pm 5) \times 10^{-3}$

Joint Analysis: Dipole Position Distribution

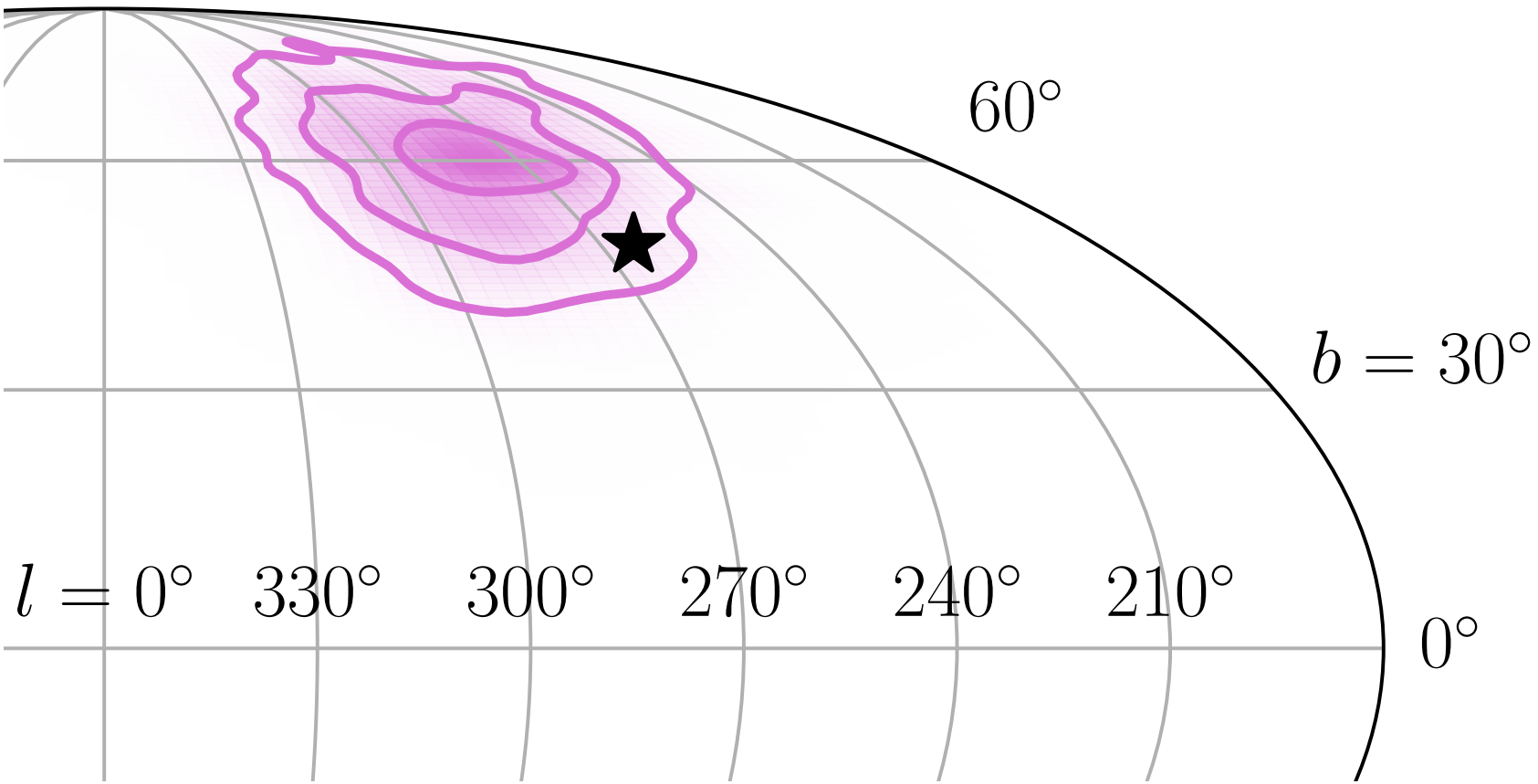

Figure 14: Projection of marginal distribution for l and b onto the sky, Galactic coordinates. ★: CMB dipole.

The Effect of Local Clustering

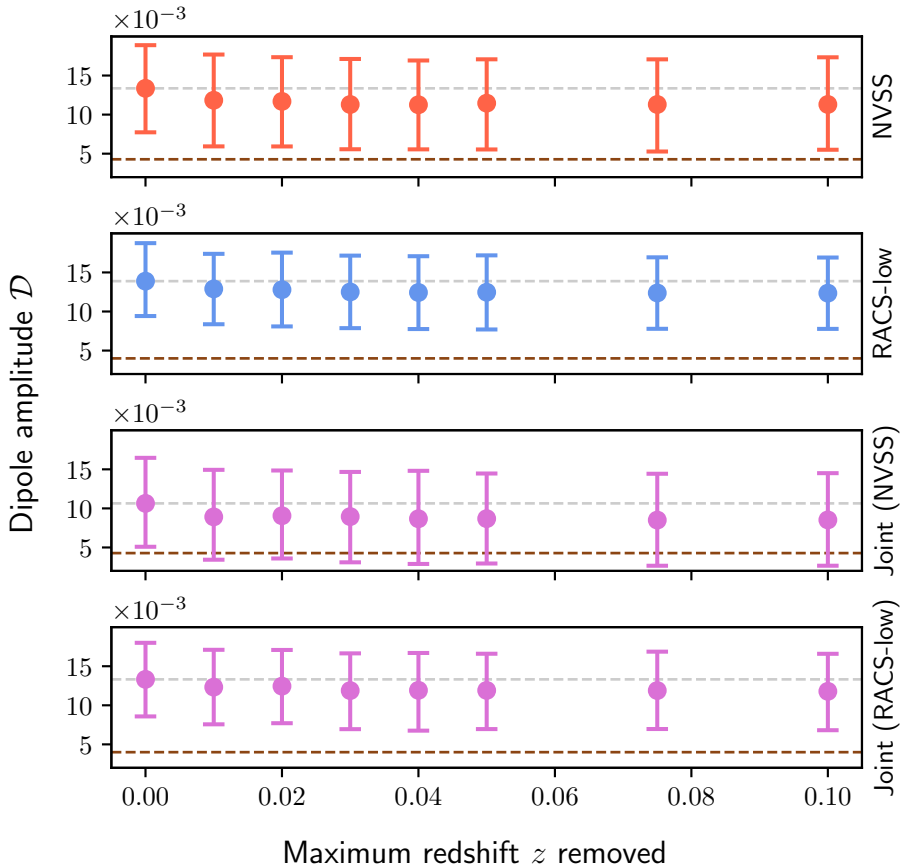

Figure 15: Inferred dipole amplitude by redshift of local source removed.

The Effect of Local Clustering

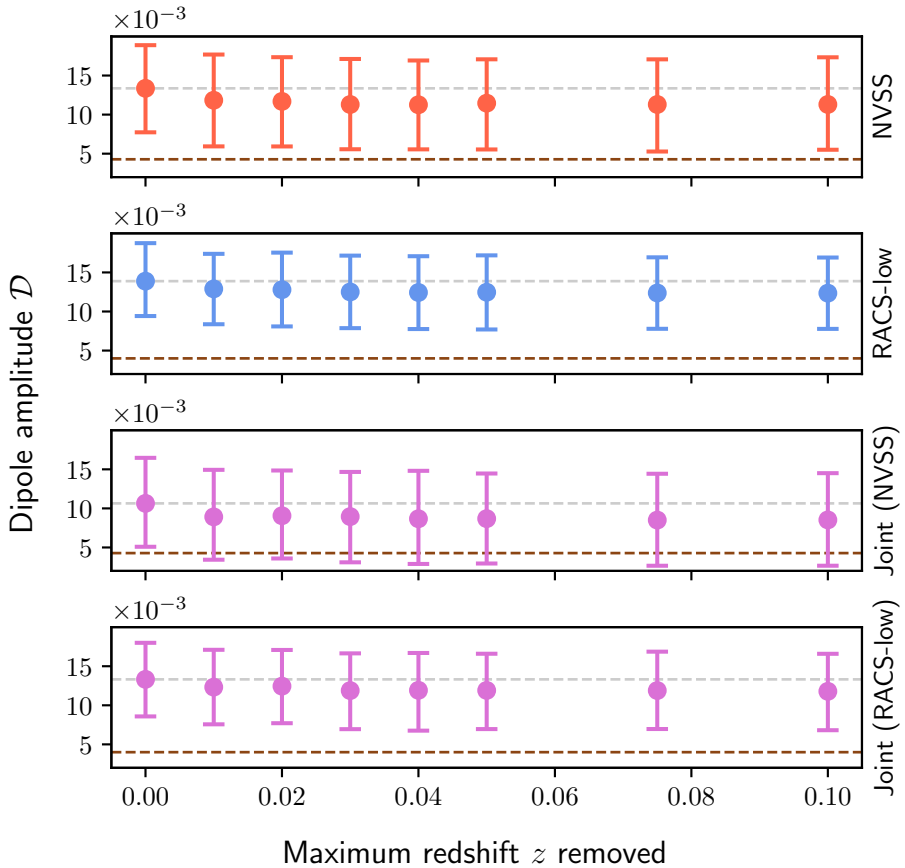

Figure 15: Inferred dipole amplitude by redshift of local source removed.

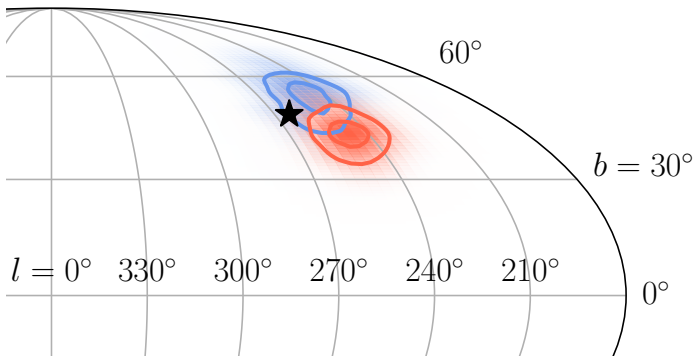

Figure 16: Inferred clustering dipole. *Star:* CMB dipole.

The Effect of Local Clustering

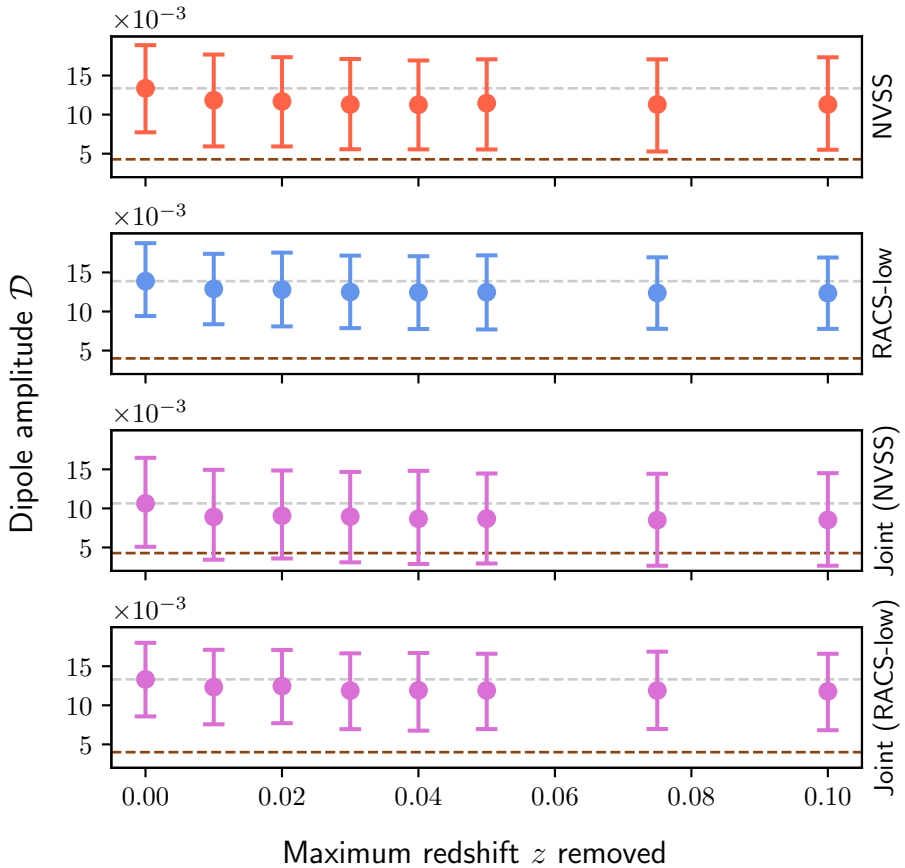

Figure 15: Inferred dipole amplitude by redshift of local source removed.

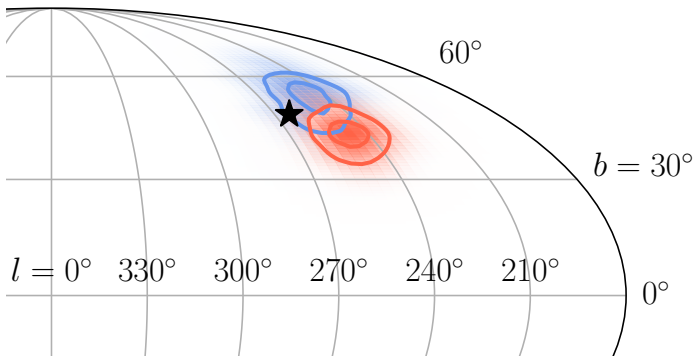

Figure 16: Inferred clustering dipole. *Star:* CMB dipole.

The clustering dipole aligns with the CMB dipole!?

NVSS and RACS Amplitudes

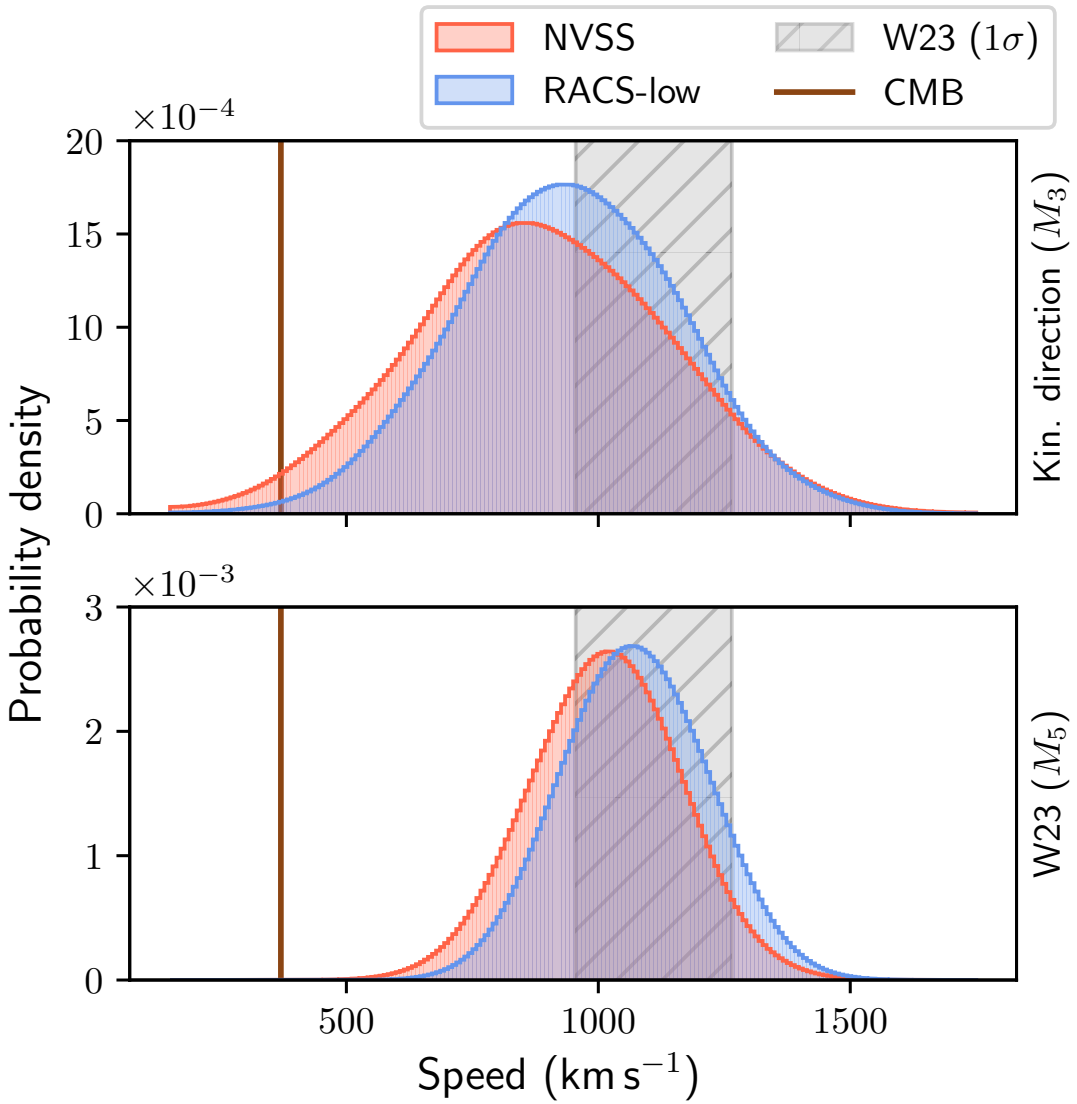

Figure 17: Marginal PDF for inferred heliocetric velocity. *Brown:* Expectation from CMB dipole. *Grey:* Results of Wagenveld et al. (2023). *Red/blue:* Our results.

The picture is somewhat similar — an amplitude $\times 2$–3 larger than the CMB expectation is preferred.

Conclusions

Summary

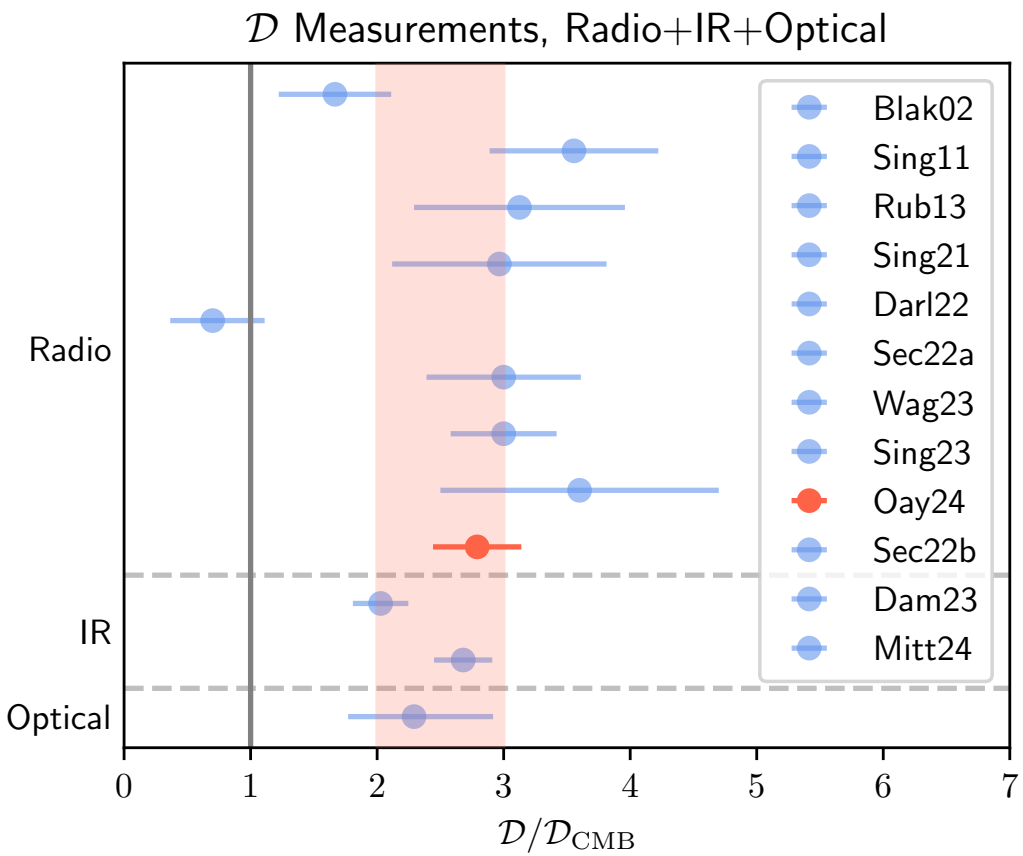

Figure 18: Literature values for $\mathcal{D}$ including results from our work (red) and other studies (blue).

There is a trend towards an excessive dipole (2 to $3 \times \mathcal{D}_{\rm CMB}$) across radio, optical and IR surveys.

This corresponds to $v \approx 1000\,\mathrm{km\,s^{-1}}$, not the $370\,\mathrm{km\,s^{-1}}$ we get from the CMB.

The Hubble H_0 tension is $\approx 10\%$. This dipole tension is 100%–200% and has reached 5σ in Secrest et al. (2021, 2022).

Outlook

- What can we do in the future?
- Radio — RACS-mid, RACS-high?
  - Need to understand systematics better
  - There are some declination-dependent effects in RACS-mid which persist in the convolved 25" catalogue
- Other dipoles? e.g. Type Ia SNe

arXiv

See the paper here!

2406.01871

What is going on? Is the cosmological principle wrong? Or are there other systematics?

References

Dam L., Lewis G. F., Brewer B. J., 2023, MNRAS, 525, 231

Ellis G. F. R., Baldwin J. E., 1984, MNRAS, 206, 377

Mittal V., Oayda O. T., Lewis G. F., 2024, MNRAS, 527, 8497

Planck Collaboration et al., 2020, A&A, 641, A4

Secrest N. J., von Hausegger S., Rameez M., Mohayaee R., Sarkar S., Colin J., 2021, ApJ, 908, L51

Secrest N. J., von Hausegger S., Rameez M., Mohayaee R., Sarkar S., 2022, ApJ, 937, L31

Springel V., et al., 2005, Nature, 435, 629

Wagenveld J. D., Klöckner H.-R., Schwarz D. J., 2023, A&A, 675, A72